Hybrid Genetic Fuzzy Systems for Control of Dynamic Systems

A Thesis

Presented in Partial Fulfillment of the Requirements for the Degree
Master of Science in Aerospace Engineering and Engineering Mechanics

By

Nicklas Stockton, B.S. Aerospace Engineering

Graduate Program in Department of
Aerospace Engineering and Engineering Mechanics

The University of Cincinnati

2018

Master's Examination Committee:

Dr. Kelly Cohen, Advisor

Dr. Manish Kumar

Prof. George Black

Abstract

Aerospace applications are composed of many dynamic systems which are coupled, nonlinear, and difficult to control. Fuzzy logic (FL) systems provides a means by which to encode expert knowledge into a set of rules which can produce highly nonlinear control signals; this is possible because FL, like many other soft computational methods is a universal approximator. While FL systems excel at encapsulating expert knowledge bases, when coupled with genetic algorithms (GA), they can learn the knowledge base from evolutionary repetition. It is the goal of this work to present the efficacy of hybrid genetic fuzzy systems (GFS) in a variety of applications.

First, a sample problem presented at the 1990 American Control Conference is used to demonstrate the robustness of FL control as well as the utility of GAs in the learning process. The results are a controller that is far more resistant to even large changes in the plant dynamics compared to a linear controller.

The next problem applies the same approach to an elevator actuator for pitch control of an F-4 Phantom. This controller is tuned for a nominal case and ten subjected to the same plant with degraded aerodynamic coefficients. It is compared to a well-tuned PID controller.

The effort culminates in a practical application of a FL system to guide a small unmanned aerial system (sUAS) to a precision landing on a target platform moving with uncertain velocity. This was accomplished using a custom developed Python for

GFS control in conjunction with Robot Operating System (ROS) and a simulation environment called Gazebo. Heavy emphasis was placed on using only software components which an be easily implemented on popular hardware platforms. ROS was critical to meeting this goal, as well as the open source flight controller project PX4. Many unanticipated drawbacks surfaced using this approach, and are discussed in detail. A great effort was made to apply GA learning to the final controller, but the end result is a hand-tuned controller controlled which is able to perform the task admirably.

Table of Contents

Page

List of Tables

List of Figures

Chapter 1: Introduction

Fuzzy logic (FL) and genetic algorithms are members of a family of so-called soft computing methods along with neural nets (NN) and probabilistic reasoning[7]. Each of these methods has particular strengths in specific domains, but all are employed in application which require computation based on imprecise, vague, or uncertain data. In recent years, NNs have risen greatly in popularity as improvements in compute power and algorithm development have allowed their application to a wide variety of problems via their role in dep learning[12]. While FL has seen much less application in deep learning applications, it has long been shown to be particularly useful in feedback control applications of nonlinear systems[19]. FL excels at encoding expert knowlede of a human operator in machine-interpretable logic. In many cases, however, it is difficult or impossible to encode a knowledge base which is sufficient to control a system satisfactorily by hand; in these cases, a GA may be applied to tune or even learn a FL system to accomplish the task.

1.1 Fuzzy Logic

The basic component of a FL system consists of fuzzy membership sets[30], which are an extension of classical binary set theory. The advantage of fuzzy set theory is that an element may share membership across many sets simultaneously in contrast

to traiditonal set logic (see figures 1.1 to 1.2). This formal encapsulation of "fuzziness" provides a method for machine instructions to operate on imprecise values. Fuzzy sets constitute the most basic element of a FL system; they are made useful in controls application when combined with a rule base (RB).

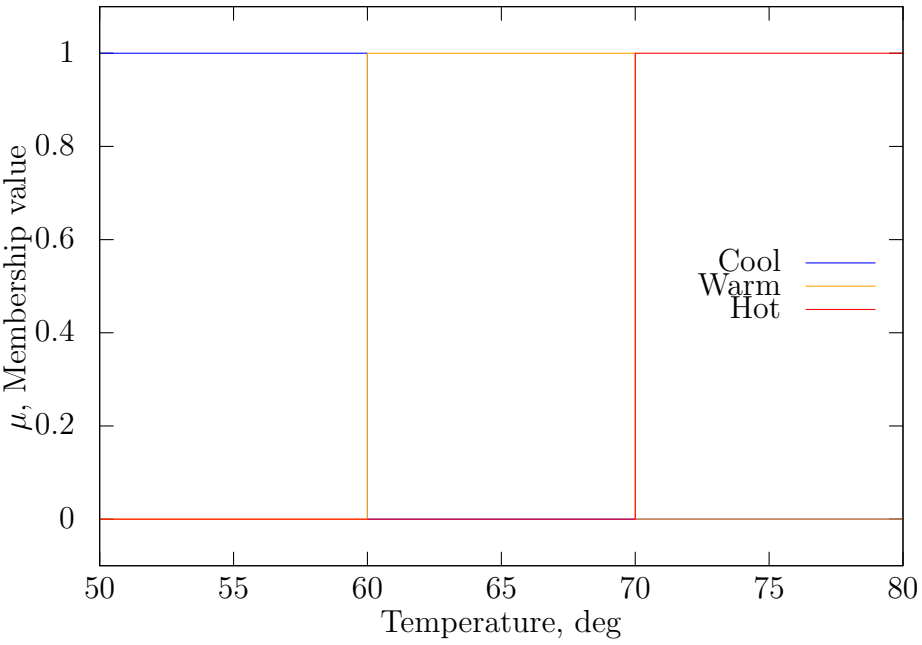

Figure 1.1: Crisp (classical) logic set transitions are discrete and abrupt

A fuzzy inference system (FIS) is a control system built on the basic principles of fuzzy logic[17][16]. It can take an arbitrary number analog inputs and map them to a set of logical variables ranging from 0 to 1. This mapping is performed by membership functions (MF), which determine the degree of membership each input has to a function. Each input typically has multiple Mfs, allowing the input value (a so-called "crisp value" to be given membership in multiple sets simultaneously. The

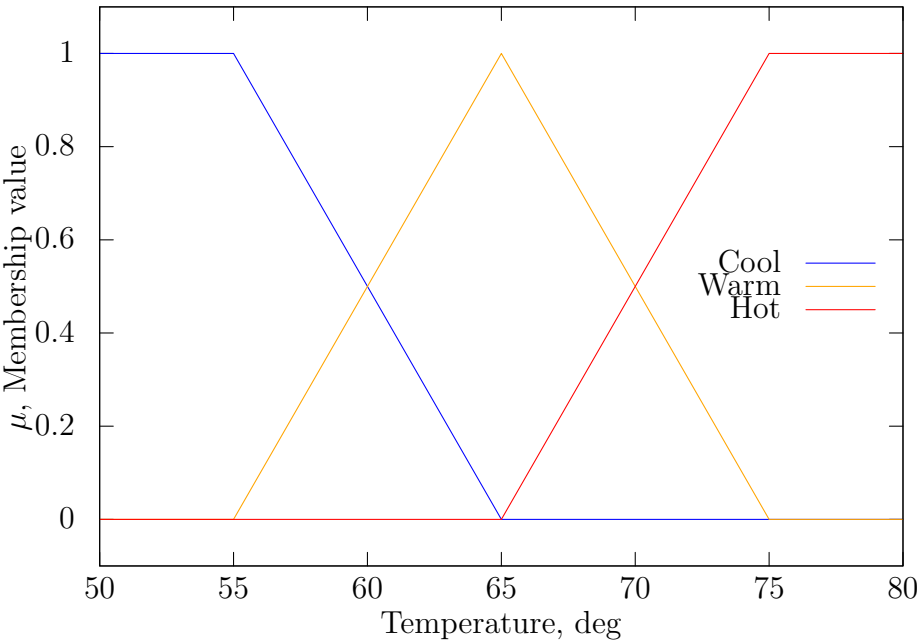

Figure 1.2: Fuzzy sets allow for multiple membership, so a value can smoothly transition from being a member of set to another.

memberships are used to make an inference about the input according to linguistic rules. The RB is composed of IF-THEN statements which determines the crisp output variable. For example, if the membership sets in figure 1.2 were to be the input to a fan controller, and the output membership functions were as they are in figure 1.3, the rules could be described as:

IF	*temperature* is	COOL,	THEN	*fan speed* is	OFF
IF	*temperature* is	WARM,	THEN	*fan speed* is	LOW
IF	*temperature* is	HOT,	THEN	*fan speed* is	HIGH

These rules can be succintly placed in a table as shown in table 1.1. This representation becomes more useful still another input is addded to the controller. By using the set of rules and the MFs, the FIS is able to determine an appropriate crisp output

given a set of crisp inputs. The FIS representation is in essence a transfer function, but a transfer function which can be arbitrarily complex. The common representation of a FIS shown in figure 1.4 shows the components of a FIS.

Table 1.1: Example rule base for a fictitious fan speed controller

Temperature	Cool	Warm	Hot
Fan Speed	Off	Low	High

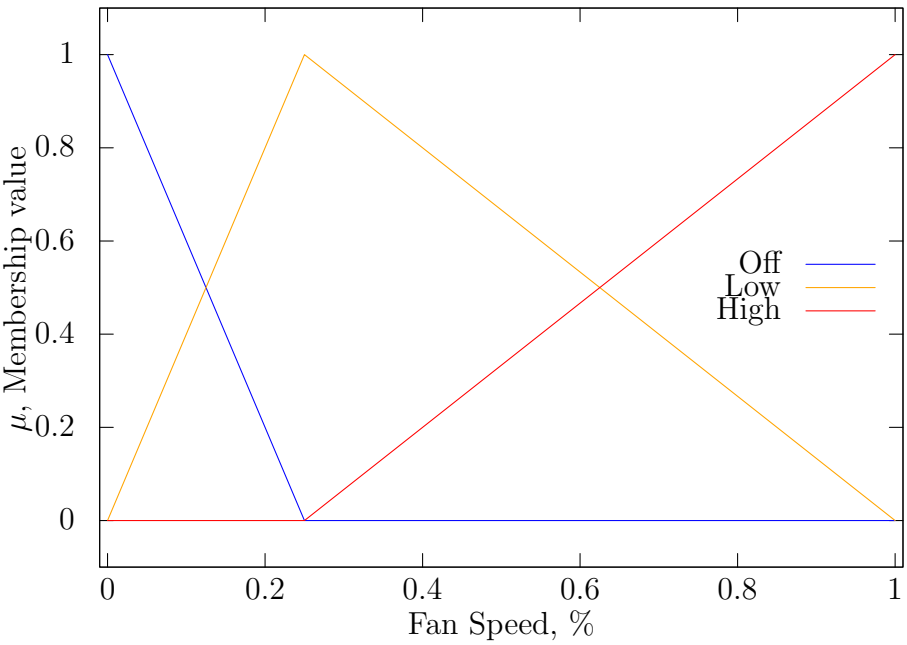

Figure 1.3: Possible output membership functions for a fan controller with figure 1.2 as the input.

One limiting constraint of FL systems is manifested in a type of state explosion. As the number of inputs, specifically the number of input MFs, increases, the number

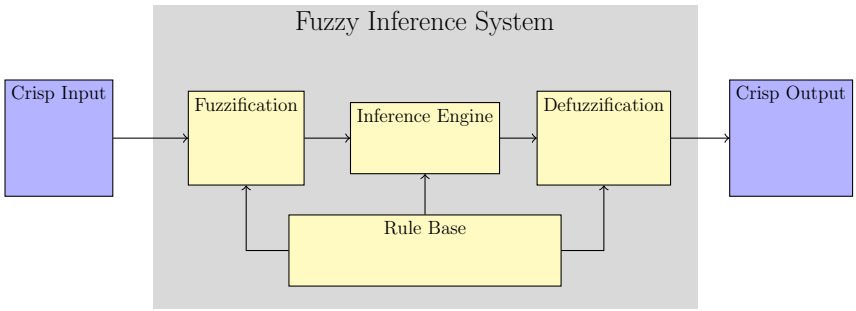

Figure 1.4: Visual representation of a fuzzy inference system

of rules needed to cover every case increases as the product of the number of MFs across all inputs. There have been numerous approaches to overcome this problem such as cascading small FISs together[10], developing more robust methods to guide convergence[13] or using approximate fuzzy rule bases[7]. The approach taken in this work, however, has been to employ GA techniques to tune the MFs or even learn the entire knowledge base. The dynamic systems being controlled in this research are adequately small that no special state reduction was deemed necessary in most cases.

1.2 Genetic Algorithms

Genetic algorithms are an evolutionary computing strategy used in optimization and search problems. GAs have been used in many search and optimization problems[2]. Their effectiveness comes from the combined ability to explore and exploit. The exploration of of even large search spaces is made possible with large populations of candidate solutions which are stochastically sampled across the whole space. Candidates are ranked according to a fitness function and recombined together to create the next generation. The algorithms exploits learnings in the selection process, favoring recombination of candidates which ranked well according to the fitness

function. In order to maintain gene pool diversity, random mutation is introduced into each generation as it is created. This process is illustrated in figure 1.5. Due to te stochastic nature of the algorithm, it is not guaranteed to provide an optimal solution and may converge on a local optimum, but careful selection of hyper parameters such as population size, mutation rates, recombination methods, and random candidate injection can circumvent these deficiencies somewhat. As the goal of a GA is to maximize some defintion of a reward, they are commonly employed in reinforcement learning applications[27].

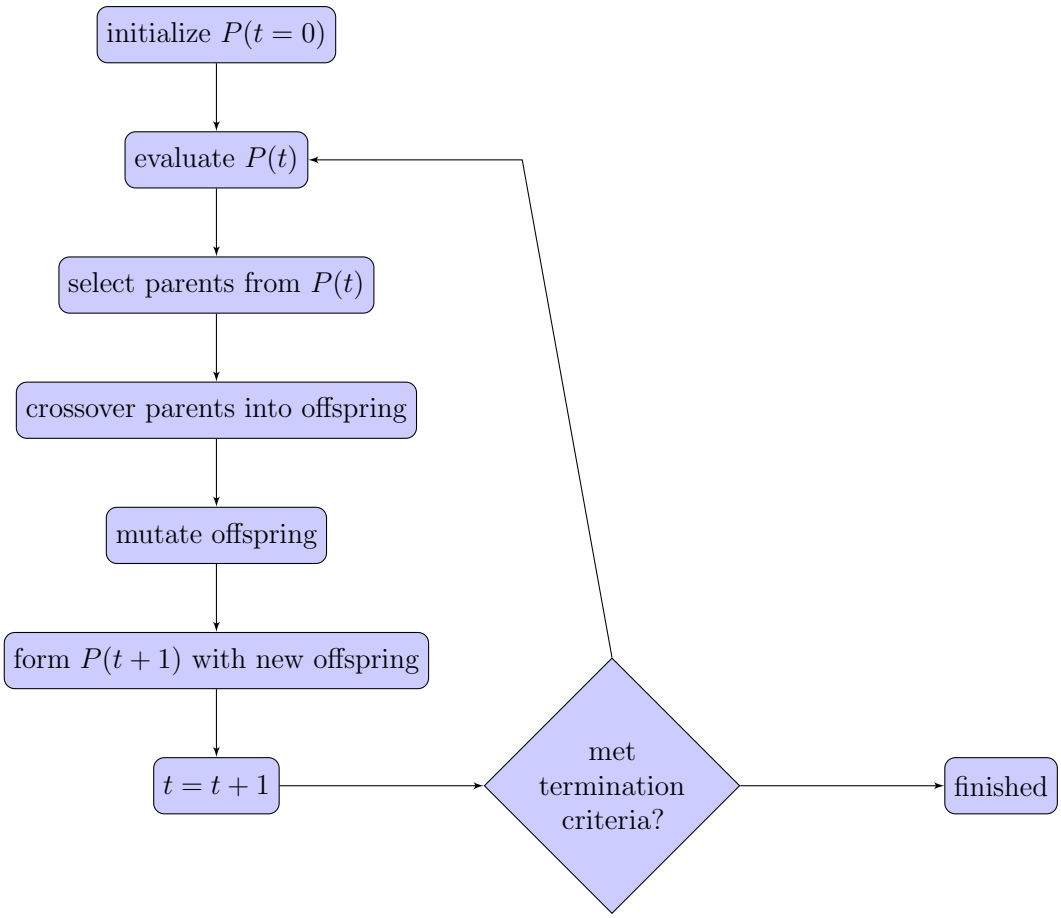

Figure 1.5: Block diagram describing genetic algorithm

Since the fitness function is the sole driver of the algorithm and the solution it provides, great care must be taken in formulating a fitness function. In robotics applications in particular, formulating a fitness which adequately encapsulates complex outcomes can be a difficult task[8]. This issue will be revisited a number of times throughout the course of this work.

Another major consideration when utilizing a GA is how to represent or encode a candidate solution for optimzation. A particularly simple method is to use a binary encoded format[7], but this increases the distance between the candidate in its usefule form (phenotype) and its encoded form (genotype) for many real-values problems[5]. A genetic encoding of a FIS is an inherently heterogenous structure with real values describing the MFs and discrete classes describing the RB. The genetic operator chosen for a specific genotype will depend on its representation; ideally, the mapping between genotype and phenotype will be one-to-one such that the combination of two genes will produce a candidate which performs similarly two its parents. This allows the GA to properly exploit its inherent learning and converge on a solution.

1.2.1 Genetic Operators

The GA advances by applying operations to the chromosome candidates in its population. The genetic operations employed in this work are crossover, mutation, and randomization. Crossover is the operation which allows the genes from two chromosomes to mix and create new children. If the chromosomes are binary encoded or discrete valued, the crossover method is generally single-, double-, or n-point crossover. This involves randomly selecting a point in the encoding string to "cut" the

chromosomes and swap the tails for single-point, or sections for n-point. Figure 1.6 demonstrates this process.

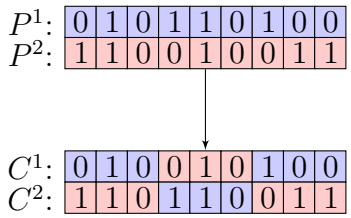

Figure 1.6: Double point crossover for binary or discrete valued chromosome.

For real-values chromosome strings, the crossover methods can be much more complex and more closely related to solution space. Throughout this work variations on flat crossover will be employed as the main crossover operation for real-valued portions of the chromosomes[7]. Using this method, a new gene is created from its parents by drawing a real value from the interval between the parent genes using a uniform distribution. In many situations, it becomes simpler to write code which always produces two children from a pair of parents; in these cases, the other gene from a parent interval is selected to be the complement of the first. Given parents, $P^1 = \{p_1^1, p_2^1, \ldots, p_n^1\}$, $P^2 = \{p_1^2, p_2^2, \ldots, p_n^2\}$, children $C^1 = \{c_1^1, c_2^1, \ldots, c_n^1\}$, $C^2 = \{c_1^2, c_2^2, \ldots, c_n^2\}$ are created such that:

$$c_i^1 = \lambda p_i^{min} + (1 - \lambda) p_i^{max} \tag{1.1}$$

$$c_i^2 = (1 - \lambda) p_i^{min} + \lambda p_i^{max} \tag{1.2}$$

where $p_i^{max} = \max(p_i^1, p_i^2)$ and $p_i^{min} = \min(p_i^1, p_i^2)$. An extension, *BLX-*$\alpha$ crossover, is used to expand the selection region beyond the interval between the parents to allow the crossover function to be more exploratory[7]. This method is described in more detail in chapter 2.

Mutation for discrete-valued chromosomes consists of randomly choosing a value from the set of possible values for a number of genes in achromosome. For this work, mutation is applied to the chromosomes after crossover is applied. The number of genes in each chromosome to mutate is defined as a hyperparameter. Mutation for real-valued chromosomes is done with a non-uniform mutation rate which decreases as the generations progress. This process is detailed in chapter 2.

For each new generation of chromosomes, a small number of the best performers are preserved untouched from the previous generation to allow the best genetic material to survive. These chromosomes are called elite. All chromosomes are ranked according to their fitness to the task and used in crossover proportional to their fitness. In other words, parents are selected for mutation by drawing chromosomes from the ranked list of chromosomes using a triangular distribution. Figure 1.7 shows a distribution laid on top of a sorted population from which parents would be selected for recombination. Parents are replaced after selection so that they may reproduce many times in one generation.

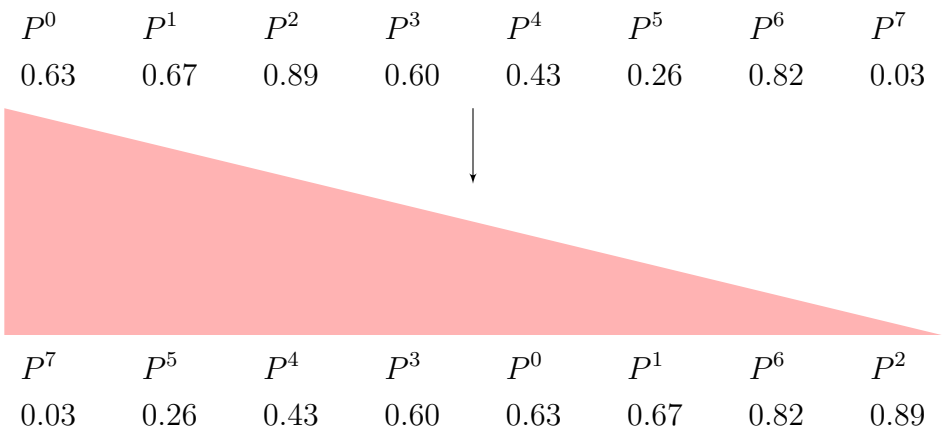

Figure 1.7: Population sorting and selection distribution overlay

1.3 Genetic Fuzzy Systems

Genetic Fuzzy Systems (GFS) here describe FL systems which have been tuned or learned using GA strategies. Tuning a GFS implies that the rule base is static, while the GA is allowed to operate on only the MF values or input/output scaling. Learning, on the other hand, implies that the RB itself is allowed to vary. For this research, except where otherwise stated, GFSs are allowed to learn the RB from scratch. In order to effectively use GAs to interact with FISs, some simplifying constraints are commonly imposed on the GFS to ease the use of genetic operators. One such constraint that is frequently used in this research is to mandate strict triangular or trapezoidal MFs. This allows the entire collection of MFs across all of the inputs to be described by either 3- or 4-tuples of sorted real values. As the GA is allowed to operate on the MFs, checks are placed to make sure that like MFs are combined in recombination and that the children contain valid MFs. All of this is eased by

constraining a GFS to only contain triangular or trapezoidal MFs. Additionally, it is assumed that the RB completely covers the input combination possibilities. This is similar to a fully connected layer of neurons in a NN. This forces the number of rules to be equal to the product of the number of MFs across all inputs; as a result of this constraint, the number of rules can quickly explode as inputs are added to the system or inputs are granularized with additional MFs. To prevent RB explosion, FISs in this work are kept minimal. Knowing the numpber of MFs, the RB can be reduced to a single string of integers, where each integer is equal to the index of one of the output MFs. Thus is in way, we can fully describe a FIS with one heterogenous string of values. For instance, the FIS illustrated in figures 1.2 to 1.3 with the RB in table 1.1 would be described completely by the list:

$$(0, 0, 55, 65)\,(55, 65, 75)\,(65, 75, 100, 100) \mid (0, 0, 0.25)\,(0, 0.25, 1)\,(0.25, 1, 1)\,[0, 1, 2]$$

where each MF tuple is grouped in (), input is separated from output with |, and the RB is in []. The genetic operations on MF paramaters are any operations which can work with real values, and the RB is constrained to n-point crossover.

1.4 Motivation and Problem Statement

This work explores the utility of using the GFS approach to exert control on dynamic systems. Because of the ability of a GFS to deal with imprecision and uncertainty, it can be an adaptive controller which can respond to changes in plant dynamics. Also, if the GFS is kept small, the trained system can be interpreted by a human operator with linguistic rules. With the rise in popularity of black box decision-making frameworks in recent years, interpretability has become a topic of

fervent research[26, 18, 31, 9]. Learning [rovides the benefit of exhibiting emergent behavior, but usually at the cost of interpretability. Genetic fuzzy systems may provide a middle ground; starting with a hand-crafted template, and then allowing a GA to learn behavior, the final model can still be assigned lingistic variables and given meaning.

This thesis is composed of a handful of problems which were approached using a GFS.

1. **Two-cart flexible system**. First, the problem of controlling a two-cart system is addressed. The system is allowed to move freely along a track with the objective of meeting, but not exceeding, a goal. This system exhibits two modes of behavior: over large distances, it behaves similar to a rigid structure; when finer control is needed in the terminal phase, the flexible body vibrations dominate the behavior. A controller is tuned to handle this system in chapter 2.

2. **F-4 Phantom Pitch Controller**. Secondly, a pitch attitude controller for the F-4 fighter jet is designed. This system is allowed to train on only a nominal flight condition, but then subjected to large degradations in plant dynamics and evaluated. The performance is shown to exceed that of a PID controller in chapter 3.

3. **sUAS Precision Landing** Finally, a controller for a small quadrotor is designed to guide the vehicle to a moving target using only visual feedback from an on-board camera. This problem is constrained by physical systems, so simulation environments, controllers, computations, and sensors are chosen such that the system will be more readily physically realized. The benefits and shortcomings

of the Robot Operating System with the Gazebo simulation environment are also discussed at length. This discussion comprises chapter 4.

Chapter 2: Two-cart Flexible System

2.1 Introduction

The 1992 American Control Conference published a set of benchmark problems to explore the capabilities of modern control techniques[29]. The second stated problem solicited solutions to the stabilization of a two-body spring mass system which was robust to uncertain masses and spring constants. A great number of solutions were conceived which performed well[28]. Cohen et. al [6] proposed a solution using fuzzy logic which is superior to all others surveyed with respect to both robustness and control effort. A variation on the same problem is addressed here. The carts are allowed to move in one dimension down a track. The carts are initially stationary, but are to be moved to a target distance without exceeding an upper limit. This system is controlled using a single FIS. The plant model masses are then changed significantly and the controller is retrained. The result is a system which can be quickly trained to accomodate new plant dynamics.

2.2 Coupled Spring-Mass Simulation Model

A simulated environment is necessary to test the efficacy of the proposed FIS. The simulation consists of two cars connected by a spring; this system is expected

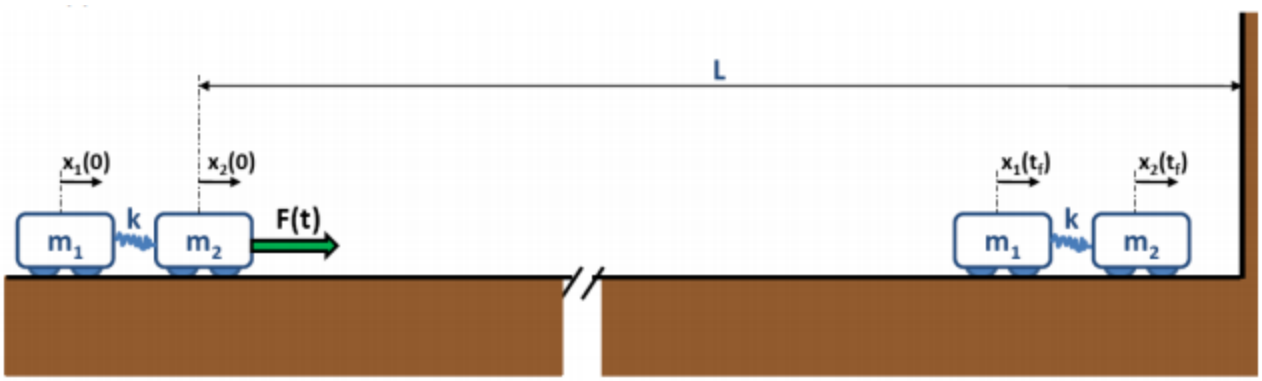

Figure 2.1: Diagram of two rigid bodies connected by a spring traversing distance L in minimum time.

to traverse a given distance as quickly as possible without exceeding a certain bound represented by a wall. The system is propelled by a force on the leading car which represents the actuating output of the controller. At each time instant, the controller must determine how much force to exert on the carts, and in which direction, to get as close as possible to the wall in minimum time. The constants for the model are the weight of each car, the spring constant, and the distance which must be traversed to the wall. A diagram of the simulation is shown in figure 2.1.

$$m_1 = 1\,\text{kg}, \quad m_2 = 2\,\text{kg}, \quad K = 250\,\frac{\text{N}}{\text{m}}, \quad L = 100\,\text{m}$$

The modeled system contains displacement and velocity sensors on each cart; therefore, the four inputs to the FIS are the distances traveled and the velocities of both carts. These inputs represent the state vector of the system. The output of the controller is the force, $F(t)$, applied to cart 2, limited to $\pm 1\,\text{N}$. At each time step of

the simulation, the FIS uses the four inputs to determine the force which must be exerted according to a fuzzy rule base.

$$\text{Input}: \quad \vec{y}(t) = \begin{bmatrix} x_1(t) \\ x_2(t) \\ \dot{x}_1(t) \\ \dot{x}_2(t) \end{bmatrix}$$

$$\text{Output}: \quad |F(t)| \leq 1\,\text{N}$$

At time $t = 0$, both carts are at rest at position $x = 0$. The maximum allowed runtime of the simulation is 500 s. The system requirement for the final condition is that neither cart exceeds 100 m and should be at rest with negligible oscillation.

$$\vec{y}_0 = \begin{bmatrix} 0\,\text{m} \\ 0\,\text{m} \\ 0\,\frac{\text{m}}{\text{s}} \\ 0\,\frac{\text{m}}{\text{s}} \end{bmatrix}, \quad \vec{y}(500) = \begin{bmatrix} < 100\,\text{m} \\ < 100\,\text{m} \\ 0\,\frac{\text{m}}{\text{s}} \\ 0\,\frac{\text{m}}{\text{s}} \end{bmatrix}$$

The acceleration of cart 1 is determined by the displacement between the two carts, the spring constant, and the mass of the cart. The acceleration of cart 2 is also a function of these parameters as well as the control force. The equations of motion for the system are represented by simple second-order differential equations.

$$\text{Cart1}: \quad \ddot{x}_1 = \frac{K}{m_1}(x_2 - x_1) \tag{2.1}$$

$$\text{Cart2}: \quad \ddot{x}_2 = \frac{K}{m_2}(x_1 - x_2) + \frac{F}{m_2} \tag{2.2}$$

2.2.1 Data Evaluation

The efficiency of a FIS's control of the system is based upon the amount of time it expends traversing the distance to the wall and how close the carts are to the wall

when they settle. Any breach of the wall results in immediate system failure. A cost function, J, is defined by the settling time t_f, the time taken to settle within 1 m of the wall and the steady state error, the distance between the leading carts and the wall. The control system that produces the lowest J value will be proven to be the most fit solution for the simulation.

$$t_f = |L - \bar{x}(t_f)| \leq 1\,\mathrm{m} \tag{2.3}$$

$$J = \frac{t_f}{100} + 2[L - x_2(500)] \tag{2.4}$$

where the constants 100 and 2 are scaling factors. In order to provide a frame of reference for the performance of any control system, the theoretical limits of the simulation were calculated to provide a lower bound for the value of Eq. (2.4). Assuming a single rigid body assembly with no dynamic coupling, the model is greatly simplified to a single equation where the acceleration of the body is a function of only the control force.

$$\ddot{x} = \frac{F}{M} \tag{2.5}$$

where M is the total mass of the system. The total mass of the system is 3 kg, whereas the maximum input force is limited to 1 N, rendering Eq. (2.5)

$$\ddot{x} = \frac{1\,\mathrm{N}}{3\,\mathrm{m}} = \frac{1}{3}\,\frac{\mathrm{m}}{\mathrm{s}^2}$$

as the maximum acceleration. Given this acceleration and the distance to be traversed to the wall, the minimum time to complete the trip can be calculated. There are, however, two scenarios to consider.

1. Applying maximum force over the entire distance and instantaneously stopping the carts at (but not touching) the wall provides an absolute, if unfeasible,

optimum simulation completed in minimum time. Given an initial velocity of zero and a constant accelerating force of 1 N, the traversal time is calculated. Note that once the carts have breached 99 m, the system may come to rest and be considered settled.

$$x(t) = \dot{x}_0 t + \frac{1}{2}\ddot{x}t^2, \quad \dot{x}_0 = 0$$

$$x(t) = \frac{1}{2}\ddot{x}t^2$$

Letting $x(t) = 99\,\mathrm{m}$

$$t = \sqrt{\frac{2x(t)}{\ddot{x}}} = \sqrt{\frac{2 \cdot 99\,\mathrm{m}}{\frac{1}{3}\,\frac{\mathrm{m}}{\mathrm{s}^2}}} = 24.37\,\mathrm{s}$$

2. Applying maximum force over half of the distance and then applying maximum negative force in the second half to slow the velocities of the carts to zero at the wall position.

   First half:

$$t = \sqrt{\frac{2x(t)}{\ddot{x}}} = \sqrt{\frac{2 \cdot 50\,\mathrm{m}}{\frac{1}{3}\,\frac{\mathrm{m}}{\mathrm{s}^2}}} = 17.23\,\mathrm{s}$$

   Traversing the second half and stopping at the wall takes the same amount of time, therefore the total time expended in reaching 100 m is 34.46 s; however, the interest lies in the time taken to breach the 99 m mark. The time taken to travel the last meter is 2.45 s, so the best possible time to reach the 99 m position is :

$$t = 32.19\,\mathrm{s}$$

   As this is a much more realistic scenario, this is the limit used as the benchmark in this research. Using this time to evaluate Eq. (2.4)

$$J = \frac{32.19}{100} + 2[100 - 100] = 0.3219$$

results in the minimum possible cost. The addition of harmonic oscillation and non-linear dynamics ensures that this limit will not be reached, but merely provides a standard against which a controller may be measured.

2.3 Fuzzy Inference System

The FIS built during this project uses two measured inputs: the position and velocity of cart 2. The output of the FIS is the force exerted on cart 2 at a given point in the simulation.

2.3.1 Membership Functions and Rule Base

Position

The first input variable, position, is composed of three membership functions to which it can map. The position of the car, from 0 m to 100 m, is described in human-understandable language as far away, close to, or very close to the wall. If the simulation has just begun and the cart is as far away from the wall as it can be, the "Far" membership function will map to 1 and the "Close" and "VeryClose" functions will evaluate to 0. Conversely, at the end of the traverse, as the car approaches the wall, "VeryClose" will map to 1 and "Far" to 0. "Close" may evaluate to some value in between. The membership functions are shown in figure 2.2(a). As the system predominately behaves as a rigid body on a large scale, the membership functions mirror the ideal simulation of a rigid body for the majority of the carts' travel. Each function is represented by a vector of values expressing the points at which the function switches from 0 to 1 or 1 to 0. For the FIS used in this research, trapezoidal- and triangular-shaped membership functions are utilized. Trapezoids are represented by a four-element vector as they start at 0, rise to 1, remain at 1, and finally fall to 0.

Likewise, triangular functions are expressed as three-element vectors. The parameters of the position membership functions shown in figure 2.2(a) are:

$$\text{Far}: \quad \text{Trapezoid} \begin{bmatrix} 0\,\text{m} \\ 0\,\text{m} \\ 49.8\,\text{m} \\ 50.1\,\text{m} \end{bmatrix}, \quad \text{Close}: \quad \text{Trapezoid} \begin{bmatrix} 49.8\,\text{m} \\ 50.1\,\text{m} \\ 99.9\,\text{m} \\ 100\,\text{m} \end{bmatrix},$$

$$\text{VeryClose}: \quad \text{Triangle} \begin{bmatrix} 99.9\,\text{m} \\ 100\,\text{m} \\ 100.1\,\text{m} \end{bmatrix}$$

Velocity

The second input variable, velocity, is composed of three membership functions. The velocity of the cart, within a range from $-6\,\frac{\text{m}}{\text{s}}$ to $6\,\frac{\text{m}}{\text{s}}$, can either be classified as "Negative", "Zero", or "Positive". When the simulation starts, the carts are at rest and the degree of membership to "Zero" velocity will be 1 whereas "Negative" and "Positive" will be 0. For the majority of the simulation, the carts are moving forward with a fast pace; therefore, the "Negative" membership function does not come into play until close to the very end of the simulation when the oscillatory effects dominate the motion of the cart system. It is at this point that the true dynamic nature of the system is exhibited and the controller does the most calculation in an attempt to damp the oscillations. The membership functions for $\ddot{x}_2$ are shown in figure 2.2(b).

The velocity membership function parameters are:

$$\text{Negative}: \quad \text{Trapezoid} \begin{bmatrix} -6\,\frac{\text{m}}{\text{s}} \\ -6\,\frac{\text{m}}{\text{s}} \\ -0.2792\,\frac{\text{m}}{\text{s}} \\ 0\,\frac{\text{m}}{\text{s}} \end{bmatrix}, \quad \text{Zero}: \quad \text{Triangle} \begin{bmatrix} -0.2792\,\frac{\text{m}}{\text{s}} \\ 0\,\frac{\text{m}}{\text{s}} \\ 0.2792\,\frac{\text{m}}{\text{s}} \end{bmatrix},$$

$$\text{Positive}: \quad \text{Trapezoid} \begin{bmatrix} 0\,\frac{\text{m}}{\text{s}} \\ 0.2792\,\frac{\text{m}}{\text{s}} \\ 6\,\frac{\text{m}}{\text{s}} \\ 6\,\frac{\text{m}}{\text{s}} \end{bmatrix}$$

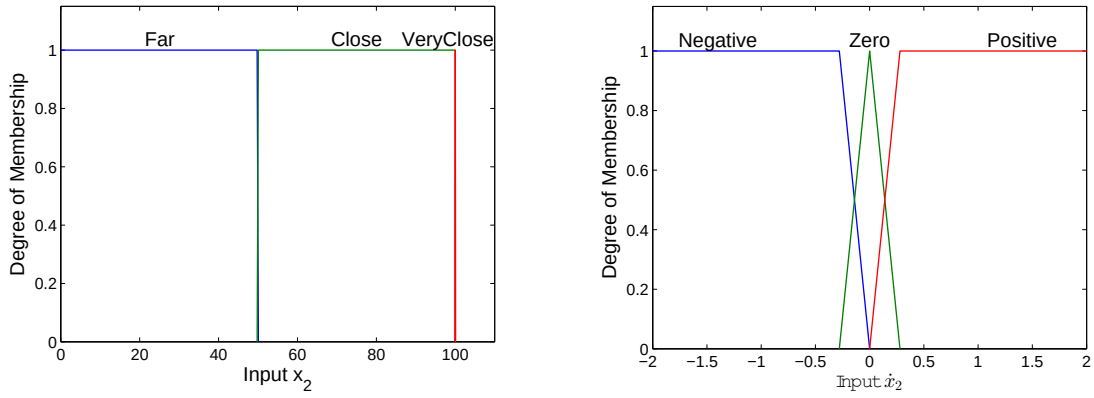

(a) x_2 membership functions

(b) $\dot{x}_2$ membership functions

Figure 2.2: Input membership functions

Rule Base

The rule base of an FIS is a series of IF-THEN (antecedent-consequent) conditions that use the membership functions of all the inputs in order to determine the output variable. There are also several membership functions for the output variable that the rule base maps to. Each of the rules has an influence on what the output of the system should be. The weight of these influences again varies from 0 to 1 and the final output value is determined by calculating the centroid of all of the rules. For instance, one rule dictates that if the car is far away then the output force should be positive and large so that the car will move towards the wall. Another rule will say that when the car is close to the wall the output force should be negative in order to slow the car down. All of these rules have influence over all input ranges determined by how the input variables map to the given membership functions in that specific rule.

The antecedent of each statement contains memberships of both input variables and the consequent maps to the output membership functions. The rules for this FIS

were developed based upon intuitive decision making. The rules developed for our FIS are shown in table 2.1.

Table 2.1: Rule Base of the Fuzzy Inference System

		Velocity Measurement		
		Negative	Zero	Positive
Position Measurement	Far	Positive		
	Close	Positive	Zero	Negative
	VeryClose	Positive	Zero	Negative
		Control Force		

Control Force

The output variable, force, is also composed of three membership functions. The output force is bounded from $-1\,\mathrm{N}$ to $1\,\mathrm{N}$ thus the membership functions allow for the output to be "Negative", "Zero", or "Positive". As the centroid of the area beneath each function is used to evaluate the control force, the upper and lower bounds are centered over 1 and -1 respectively. These functions represent the "defuzzification" stage of the FIS and these outputs are determined by evaluating each rule in the rule base (see section 2.3.1) in parallel[20]. The controller emulates bang-bang control for the majority of the simulation lifetime, sharply transitioning from full acceleration to full deceleration. As the cart system nears the wall, the oscillation damping rules will

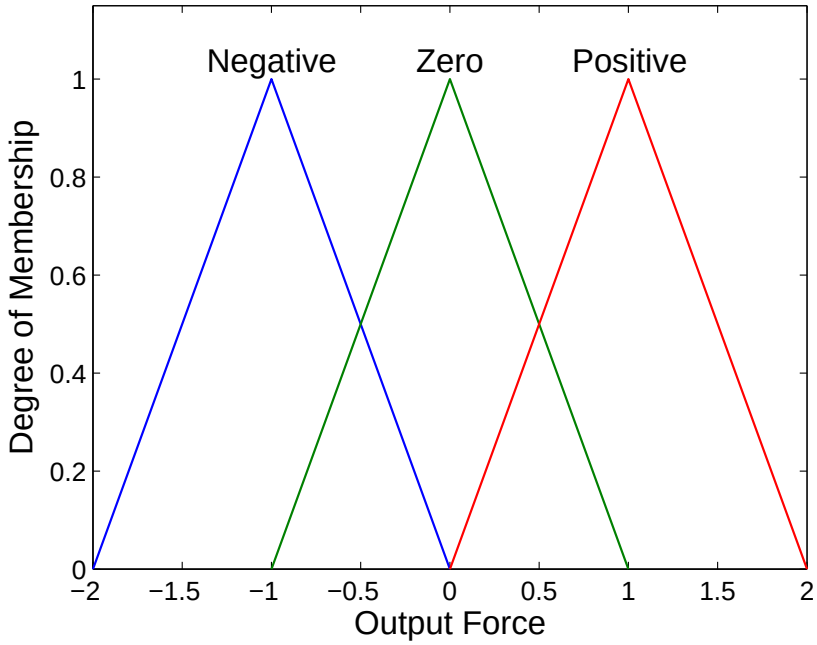

Figure 2.3: Control force membership functions.

dictate the force to apply on the system. Typically, the output force will be directed opposite to the velocity of cart 2. The membership functions for the control force are shown in figure 2.3.

$$\text{Negative}: \quad \text{Triangle}\begin{bmatrix}-2\,\text{N}\\-1\,\text{N}\\0\,\text{N}\end{bmatrix}, \quad \text{Zero}: \quad \text{Triangle}\begin{bmatrix}-1\,\text{N}\\0\,\text{N}\\1\,\text{N}\end{bmatrix}, \quad \text{Positive}: \quad \text{Triangle}\begin{bmatrix}0\,\text{N}\\1\,\text{N}\\2\,\text{N}\end{bmatrix}$$

2.3.2 Simulation Performance

The efficiency of this FIS was determined by using it as the control mechanism in the simulation. The goal was to approach the realistic theoretical limits calculated above and reach this goal with minimum force. table 2.2 shows the settling time, final position of cart 2 and the calculated J value for the controller's performance.

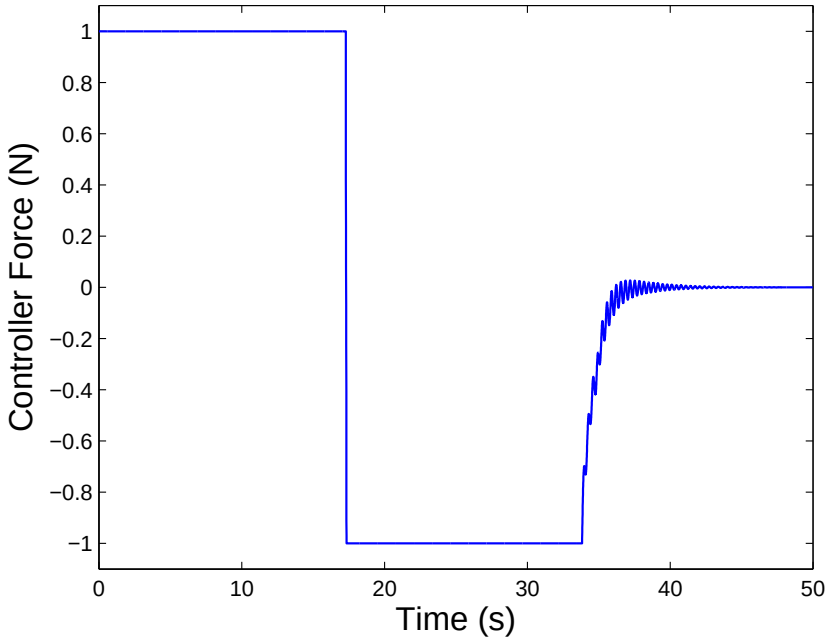

Figure 2.4: System control force over time.

Figure 2.4 shows the controller's output force over time for each step of the simulation. The controller's output force is much lower than previously tested fuzzy solutions as well as an optimal linear controller.

It is clear that the controller expends less energy than a traditional bang-bang type controller would in the oscillation damping process. It can be seen that the FIS responds quickly to control needs and applies the needed force with low-latency.

Much work was done to hand-tune this controller to perform optimally, thus the work was undertaken to develop a genetic algorithm to produce similar results autonomously. Automating the tuning process ultimately produces a controller which is nearly as good as the hand-tuned controller, but requires little to no effort from the programmer.

Table 2.2: Results from implemented FIS.

t_f	$x_2(500)$	J
32.303 s	99.999 821 m	0.32328

2.4 Genetic Algorithm

The performance of the FIS depends directly on the value of each parameter of the membership functions. These values were hand-tuned by a time-consuming process of trial and error. To quicken this process, a genetic algorithm was utilized to autonomously tune the membership functions and approach an optimal solution.

A genetic algorithm is a computational mechanism which imitates evolutionary behavior to achieve optimality. It consists of a population of individuals which undergoes a process similar to natural selection, reproduction, and mutation over the course of a number of generations[7]. Selection is attained by evaluating the fitness of each individual according to a fitness function. For the purposes of this research, each individual represents a FIS and the fitness function is simply the cost function used earlier. The individual which most effectively minimizes the cost function is considered most fit for the control environment.

In order to manipulate the FIS structure in an algorithmic manner, it is necessary to represent it as a genetic individual. Since the values of the parameters of the membership functions of the FIS have significant impact on the control performance, it was decided to manipulate only these parameters with the algorithm; however, of the thirty-one parameters which comprise this FIS model, many are trivial to the

overall performance. It is desirable to reduce the number of parameters to facilitate the optimization process.

2.4.1 State Reduction

To simplify the genetic tuning of the parameters, the symmetry of the system was exploited. The parameters were reduced from thirty-one to seven. The position membership functions were simplified to only three parameters by defining a center point (center) between far and close functions, a distance from the center point at which the far and close functions will be valued at 0 and 1 respectively (iTrap1), and half of the base of the triangular membership function which decides when the car is very close to the wall (iTriBase1). The velocity membership function parameters were reduced to two parameters by defining the one parameter for the distance from 0 that each of the membership functions reaches 1 for the negative and positive functions (iTrap2) and another to define half of the base of the zero velocity triangular membership function (iTriBase2). The output force membership functions were reduced similarly by allowing the negative and positive membership functions become trapezoidal (oTrap and oTriBase).

- Position Membership Function Parameter

$$\text{Far}: \quad \text{Trapezoid} \begin{bmatrix} 0 \\ 0 \\ (center - iTrap1) \\ (center + iTrap1) \end{bmatrix}, \quad \text{Close}: \quad \text{Trapezoid} \begin{bmatrix} (center - iTrap1 \\ (center + iTrap1) \\ 99.9 \\ 100 \end{bmatrix},$$

$$\text{VeryClose}: \quad \text{Triangle} \begin{bmatrix} (100 - iTriBase1) \\ 100 \\ (100 + iTriBase1) \end{bmatrix}$$

- Velocity Membership Function Parameters

$$\text{Negative}: \quad \text{Trapezoid} \begin{bmatrix} -6 \\ -6 \\ (0) - iTrap2) \\ 0 \end{bmatrix}, \quad \text{Zero}: \quad \text{Triangle} \begin{bmatrix} (0 - iTriBase2) \\ 0 \\ (0 + iTriBase2) \end{bmatrix},$$

$$\text{Positive}: \quad \text{Trapezoid} \begin{bmatrix} 0 \\ (0 + iTrap2) \\ 6 \\ 6 \end{bmatrix}$$

- Control Force Membership Function Parameters

$$\text{Negative}: \quad \text{Trapezoid} \begin{bmatrix} -2 \\ (-1 - oTrap) \\ (-1 + oTrap) \\ 0 \end{bmatrix}, \quad \text{Zero}: \quad \text{Triangle} \begin{bmatrix} (0 - oTriBase) \\ 0 \\ (1 + oTriBase) \end{bmatrix},$$

$$\text{Positive}: \quad \text{Trapezoid} \begin{bmatrix} 0 \\ (1 - oTrap) \\ (1 + oTrap) \\ 2 \end{bmatrix}$$

These state reductions allow an individual to be defined by a single vector of seven variables.

- Individual Definition

$$\begin{bmatrix} iTrap1 \\ center \\ iTriBase1 \\ iTrap2 \\ iTriBase2 \\ oTrap \\ oTriBase \end{bmatrix}$$

2.4.2 Population Initialization

An initial population is generated by assigning random values to each of the individual parameters within given ranges. iTrap1, iTriBase1, and oTriBase are allowed to vary between 0.05 and 1. iTrap2 and iTriBase2 are allowed to vary between

0.05 and 2. Center values fall between 45 and 55, and oTrap between 0.05 and 0.95. Twenty individuals comprise a population. Each individual is evaluated for fitness and brought up for selection to produce a new generation.

2.4.3 Parent Selection and Reproduction

A new generation consists of three individuals which remain unchanged from the previous generation, called elite children, ten individuals which are created from recombination of two parents, five individuals which are created from mutating recombined children, and two individuals randomly defined from the previously defined ranges.

Parents are selected by selecting the three best fit individuals to both become parents and elite children. Seven more parents are selected by randomly choosing three individuals from the remaining population, selecting the most fit, and returning the other two. This tournament style of selection is repeated until all parents are selected.

Reproduction occurs by blended crossover process with an α modification (BLX-α), by selecting a new parameter x_i' from the range $[x_{min} - I\alpha, x_{max} + I\alpha]$, where

$$x_{min} = min(x_i^1, x_i^2) \quad \text{and} \quad x_{max} = max(x_i^1, x_i^1)$$

Parents are defined as

$$C^1 = (x_1^1, x_2^1, \cdots, x_7^1) \quad \text{and} \quad C^2 = (x_1^2, x_2^2, \cdots, x_7^2)$$

$$I = \frac{x_{max} - xmin}{b_i - a_i}$$

$$\alpha = min(d^1, d^2)$$

$$d^1 = x_{min} - a_i \quad \text{and} \quad d^2 = b_i - x_{max}$$

The interval $[a_i, b_i]$ is the parameter-specific range. This mechanism allows the algorithm to create a child from two parents which is a blend of both parents, while still expanding the search space. As a population generally converges on a solution, so too do the children of the population.

2.4.4 Mutation

Five of the recombined children are selected by random sampling and then two randomly sampled parameters are selected from each of these child for mutation. Mutation is defined to be nonuniform such that the mutation has a smaller effect in later generations as follows:

$$x_i' = \begin{cases} a_i + \Delta(t, x_i - a_i), & \text{if } \tau = 0 \\ b_i - \Delta(t, b_i - x_i), & \text{if } \tau = 1 \end{cases}$$

where τ represents a coin flip such that $P(\tau = 1) = P(\tau = 0) = 0.5$

$$\Delta(t, x) = x(1 - \lambda(1 - \frac{t}{t_{max}})^b)$$

where t is the current generation, and t_{max} is the maximum number of generations. The variable λ is a random value from the interval $[0, 1]$. The function Δ computes a value in the range $[0, x]$ such that the probability of returning a zero increases as the algorithm advances. The value of b determines the impact of the time on the probability distribution of Δ. The value of b is set to 1.5 for algorithm for this research.

Two additional children are added to the population by random selection from the ranges in order to ensure that the search space is sufficiently large.

Table 2.3: Final Results from algorithm-generated FIS

t_f	$x_2(500)$	J
32.308 s	99.999 999 m	0.32311

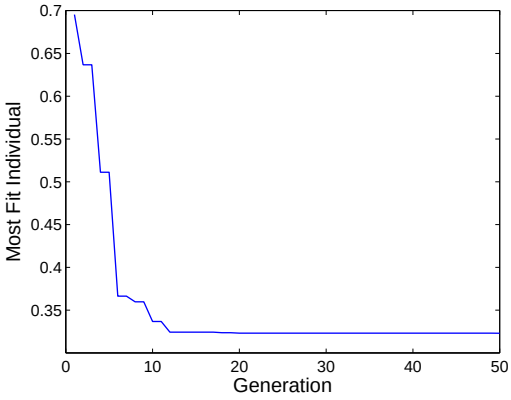

(a) Best fit individual by generation.

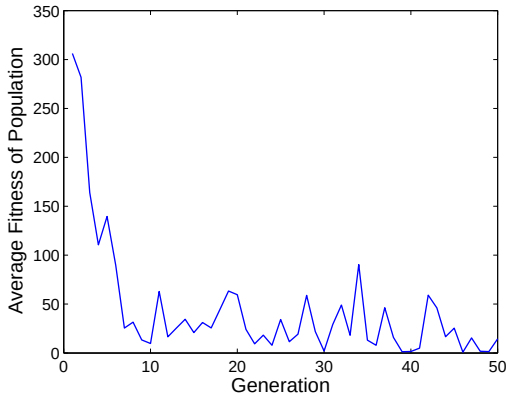

(b) Individual fitness average by generation.

2.5 Results

Running the algorithm for 50 generations yields a FIS which performs as well as the hand-tuned FIS from section 2.3.2. This result converges out of the evolution process quickly as can be seen in figure 2.5(a). Though the algorithm finds a near optimal solution quickly, it continues to search similar solutions, selecting the best individuals each time to produce progressively better fit children each generation. Figure 2.5(b) shows the average fitness of generation. It is clear from this plot that the algorithm produces many unfit children in its search for optimality. This satisfies the need of a good algorithm to expand the search area to eliminate premature convergence.

The results of the performance of the most fit individual produced by the genetic algorithm are shown in table 2.3.

Table 2.4: Genetic algorithm FIS performance compared the hand-tuned FIS and rigid body limit.

	Mass 1 (kg), Mass 2 (kg)			
	1 kg, 2 kg	2 kg, 4 kg	4 kg, 8 kg	4 kg, 16 kg
Theoretical Limit	0.3191	0.4553	0.6438	0.8312
GA FIS	0.3231	0.4562	0.6579	0.8434
Hand-tuned FIS	0.3233	0.6125	5.3072	3.3240
GA Error	1.3%	0.2%	2.2%	1.5%
Hand-tuned Error	1.3%	34.5%	724.4%	299.9%

2.5.1 Genetic Adaptability

These results demonstrate the ability of the genetic algorithm to tune a FIS to near-optimal performance. All tuning and development heretofore was done with an unchanging system setup of known masses connected by a known spring. Although a robust controller[6], introducing changes to the masses of each car significantly alters the performance of the FIS as it was carefully tuned to only a certain envelope; however, utilizing the genetic algorithm to generate an optimum FIS for each new system setup is an efficient method of developing good active controllers. This is demonstrated by changing the masses m_1 and m_2 to 2 kg and 4 kg respectively. They are again changed to 4 kg and 8 kg, and finally 4 kg and 16 kg. The algorithm was deployed for each case to optimize a controller for that envelope. After fifty generations of evolution, the genetically optimized FIS performed within 3% of the theoretical rigid body limit in all four cases. These results are displayed in table 2.4.

It is easily seen in these results that the use of the genetic algorithm is advantageous in the autonomous development of near optimal FIS controllers. Given a generic

control architecture, the genetic algorithm is able to tune a FIS rapidly and accurately for a varied set of circumstances.

2.6 Conclusions

Fuzzy logic provides a robust framework for control. It has been demonstrated that proper fuzzy control is efficient and computationally inexpensive. The inherent vagueness of set membership and linguistic operation of fuzzy logic allows the controller to mimic expert human control. This superior control, however, comes with a steep cost in FIS development. Hand-tuning a FIS is time-consuming and tedious.

The use of the genetic algorithm facilitates FIS development. Once a FIS has been developed for a general type of control situation, it is relatively simple to define the FIS as a genetic element and automate the tuning through the evolutionary process. These results imply that if a general fuzzy controller is developed for a family of control situations, then a genetic algorithm can be implemented to tune each FIS to its specific task. The tuning, therefore, can be accomplished by someone with no expertise in the control of the situation. As the computation is quick, efficient control could be widely distributed due also to the low-cost of development.

Chapter 3: F-4 Pitch Attitude Control

3.1 Introduction

The main challenge of this problem lies in the fact that the flight conditions that a fighter jet experiences are wide and varied. It is not possible to design and implement an optimal controller for each one individually. In this situation, it is logical to design a controller which works near optimally for those conditions which the jet is likely to spend the bulk of its time in, but one which also works for the flight conditions at the edge of the envelope. The traditional approach for this desired behavior is to determine the PID gains for each common flight condition and perform gain scheduling to allow the controller response to be tuned to each condition. The gains are then allowed to vary between set design points according to some parameterization by some higher function so that they can smoothly and constantly "float" around to match the flight conditions. One such method is to set the PID gains from a fuzzy inference system (FIS). This paper outlines one such system for the approach condition of an F4 fighter jet. A fuzzy-PID controller was tuned for the nominal approach condition, and then applied to various other flight conditions to show its robustness. No known PID gains are used from the outset, rather, broad ranges are given to the GFS and

it is allowed to create its own universal approximator to find the gains which give optimal performance at any point.

3.2 Fuzzy PID

The plant dynamics for all scenarios have poles which are very close to the right half of the plane, meaning that this system can easily be destabilized by exerting incorrect control force. Much care needs to be taken when designing a controller for such a system. Fuzzy logic is well-suited to this task in that it will allow the control gains to move around in a way which will keep the poles in the left half of the plane. The system dynamics studied here were used to control a PID and a Fuzzy controller by Bossert and Cohen[4] which will be used as a benchmark.

One large downside to fuzzy systems are that they require a significant expense of effort to tune. This task becomes even more cumbersome with an increase of membership functions, which, in turn, increase the number of rules (possibly exponentially). The FIS designer is then relegated to either drawing on a store of heuristic knowledge or experience (perhaps from an expert), or to trial-and-error iteration to incrementally improve the controller. The method used in this paper is a GA which plays the part of automating and guiding the trial-and-error process (see next section). This method effectively circumvents the difficulty of tuning a FIS, and makes the job of controlling this near-unstable system more feasible.

3.3 System Controller Design Methodology

At first, an attempt was made to utilize Simulink® and MATLAB® to design a genetic algorithm (GA) which would simulate the plant transfer functions with a

fuzzy-PID controller in the feedback loop. The GA, written in MATLAB, would call the Simulink model and evaluate the performance of the controller. This methodology presented a number of problems to the designer. The Simulink Fuzzy Logic Block seemed to slow down the execution of the control loop siginificantly, making a single simulation run up to an order of magnitude slower than one with only PID control. This shortcoming can be circumvented by using a lookup table in place of the fuzzy controller, but the overhead time needed to generate the lookup table negates the simulation speed gains.

In light of the issues with using a Simulink GA, the GA was implemented in traditional MATLAB using `ODE45` as the ordinary differential equation solver; however, due to the adaptive timestep of the solver, it is prohibitively difficult to accurately obtain error derivative and integral terms for use in the PID controller. This led the author to eventually write a simple ode solver in MATLAB which gives access to all errors at each time step, but the execution of a single simulation was expectedly and prohibitively slow.

At this point, the decision was made to implement a genetic fuzzy system using the C programming language. The author had already implemented one such system in Python and made quick work of translating it into C. This GA uses the comparable rk8pd (Runge-Kutta Prince-Dormand (8,9)) stepping function from the Gnu Scientific Library (GSL) to solve the ordinary differential equation. This method allows the user to specify some basic parameters which are desired in the final FIS, a cost function to be applied to each solution, and some basic parameters for the GA, at which point the GA starts generating and evaluating FIS's until a suitable stop condition has been met.

For the proportional gain, K_p, a SISO FIS is created which accepts only angular error as input. To calculate the integral and derivated gains, K_i, and K_d respectively, two 2-input, 1-output FISs are made. These FISs both accept the absolute error in elevator position (e_p), and also the error integral (e_i), and the error derivative (e_d) respectively.

The cost function used to evaluate each FIS was derived using the fuzzy-PID controlled dynamic system response to a step function. The cost function is obtained by simply summing the settling time and the overshoot fraction. It should be noted that likely due to some small numerical differences in the GSL solver and MATLAB's `ODE45`, the settling times reported by MATLAB are marginally slower in most cases than than what is given in table 3.1.

3.4 Results for Nominal and Other Flight Conditions

Table 3.1: Comparison table of current results with those of Bossert and Cohen

Case	T_s (s)	T_r (s)	T_p (s)	M_p (deg)	FV (deg)
Root Locus F4 Approach (Design Condition)	23.6	1.09	3.14	1.09	0.62
PID F4 Approach (Design Condition)	7.08	1.27	4.98	1.023	1.00
Fuzzy F4 Approach (Design Condition)	1.65	1.68	1.74	1.013	1.00
Fuzzy PID Approach (Design Condition)	1.86	0.26	0.66	1.396	1.00
Root Locus 50% Red in $C_{m\alpha}$ and C_{mq}	25.8	1.16	3.57	1.42	0.77
PID 50% Red in $C_{m\alpha}$ and C_{mq}	8.0	1.03	1.35	1.045	1.01
Fuzzy 50% Red in $C_{m\alpha}$ and C_{mq}	1.66	1.69	1.75	1.014	1.00
Fuzzy PID 50% Red in $C_{m\alpha}$ and C_{mq}	1.87	0.25	0.66	1.428	1.00

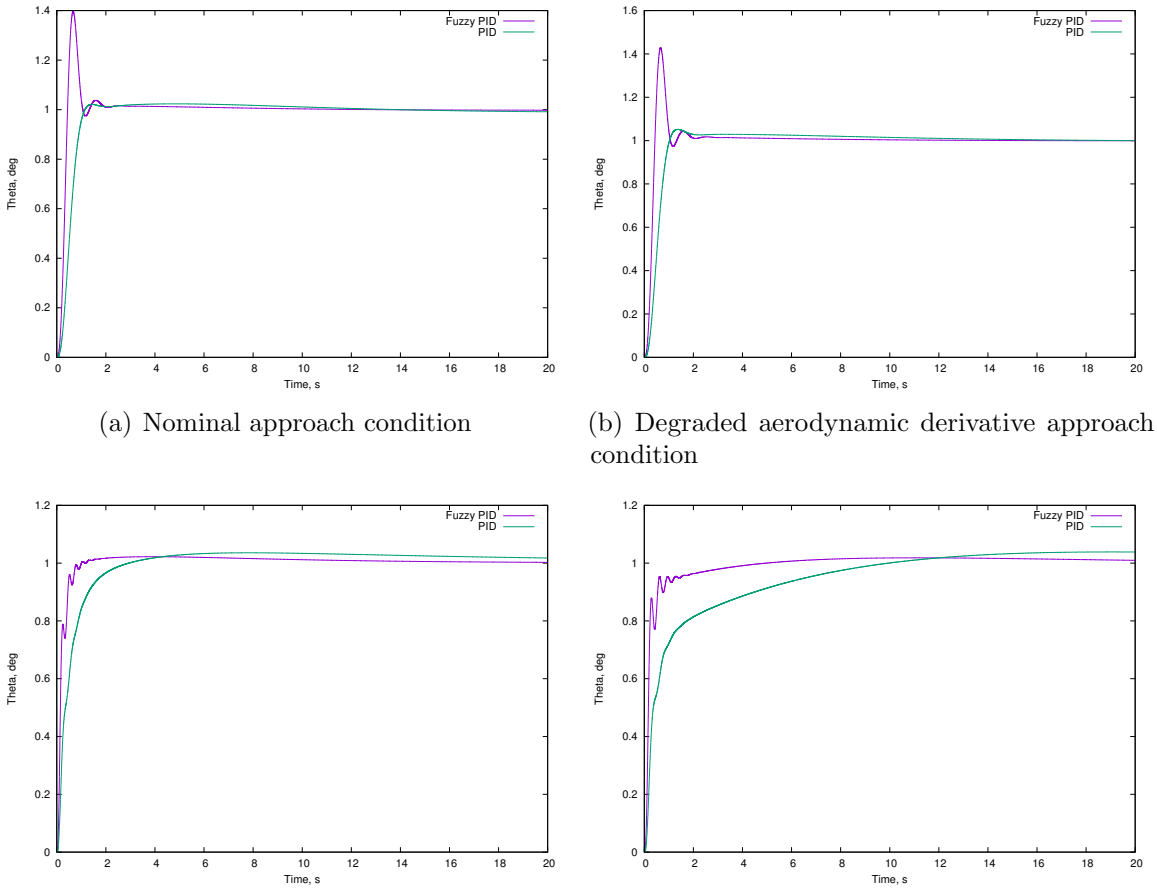

(a) Nominal approach condition

(b) Degraded aerodynamic derivative approach condition

(c) Subsonic cruise condition

(d) Supersonic cruise condition

Figure 3.1: Step response for various flight conditions. Note the increased overshoot for nominal conditions from the Fuzzy-PID controller.

Table 3.2: Resulting FIS response from GA with modified cost function

Case	T_s (s)	T_r (s)	T_p (s)	M_p (deg)	FV (deg)
Fuzzy PID Approach (Design Condition)	4.96	0.34	1.43	1.031	1.00
Fuzzy PID 50% Red in $C_{m\alpha}$ and C_{mq}	4.47	0.33	0.66	1.043	1.00

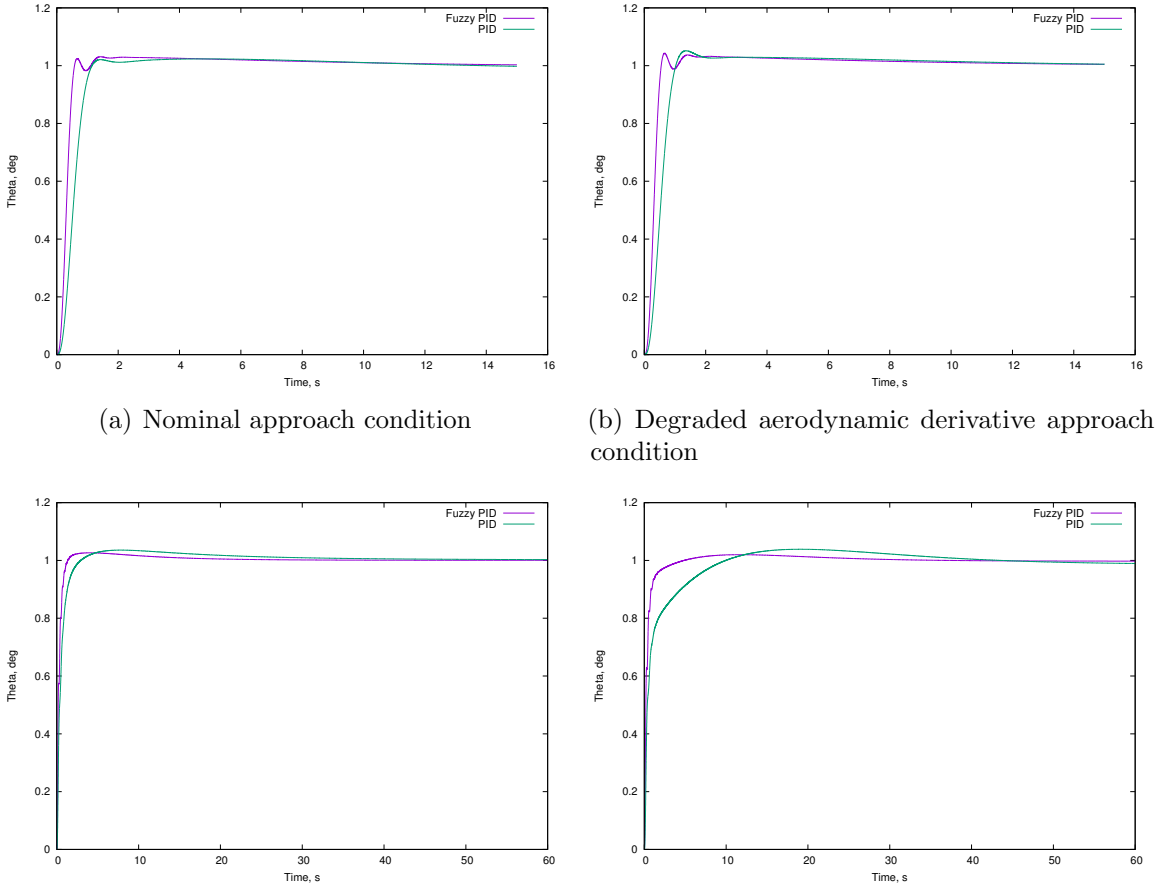

(a) Nominal approach condition

(b) Degraded aerodynamic derivative approach condition

(c) Subsonic cruise condition

(d) Supersonic cruise condition

Figure 3.2: Step response for various flight conditions. Note the significantly decreased overshoot for nominal and degraded flight conditions.

Table 3.3: Comparison of response times for subsonic and supersonic cruise conditions for original and modified cost function. Modifying the cost function showed no improvements for this set of conditions, rather only proved to slow the response time with no gain in overshoot.

Case	T_s (s)	T_r (s)	T_p (s)	M_p (deg)	FV (deg)
Subsonic Cruise (Orig. Cost)	0.93	0.38	3.91	1.022	1.00
Supersonic Cruise (Orig. Cost)	3.84	0.73	11.10	1.018	1.01
Subsonic Cruise (Mod. Cost)	7.97	0.59	4.09	1.026	1.00
Supersonic Cruise (Mod. Cost)	15.53	0.73	11.74	1.020	1.00

3.5 Discussion

As can be seen from table 3.1 and figures 3.1(a) to 3.1(b), the overshoot which comes at a cost of decreased settling time is unacceptable. This is a product of defining a cost function which under-penalizes overshoot and over-emphasizes settling time alone. The results were retained as part of the project to show both the benefits and shortcomings of using a GA t tune a FIS. That is, the FIS will be shaped to minimize the cost of whatever function is provided, whether or not the desired outcome is truly reflected by that function. For this reason, much care is needed when choosing a cost function to be minimized. The GA was given a new cost function which put a higher premium on overshoot and given a FIS to optimize for the plant. The results from this run are shown in table 3.2 and figure 3.2. As can be seen from table 3.2, the settling time of the step response is significantly slower, but the overall response is arguably better that figure 3.1 due to the reduced overshoot. Additionally, though not nearly as good for the nominal and degraded flight conditions as was Bossert and Cohen's solution, the response for the subsonic and supersonic cruise conditions show arguably better performance than theirs.

3.6 Conclusion

It has been shown that fuzzy augmented systems can greatly improve the behavior of controllers. Where traditional control logic can attain reasonable performance for only nominal and near-nominal conditions, fuzzy logic can extend the performance gains across a much wider set of conditions. It is also clear the effect the cost function can have on the result of the controller. The oversimplistic cost function of settling time alone produces undesirable results in the rest of the response. Careful consideration

needs to be taken in cost function development. It was only after modifications to the cost function were made that the response confromed to a more desirable shape.

Chapter 4: Fuzzy Landing

4.1 Introduction

With the ever-increasing proliferation of small unmanned air vehicles (sUAVs) and their use in commercial and emergency response applications, there is a growing need for intelligent, reliable control methodologies to safely manage their navigation, especially in possibly congested areas such as disaster areas or urban centers. Commercial delivery companies are moving towards an automated model with reduced human operator intervention to increase the efficiency of their deliveries. One such model consists of a vehicle-based sUAV which departs from the delivery vehicle to make a delivery to a remote residence. Upon completing the delivery, the sUAV returns to the vehicle and docks to receive additional packages. Considering the small target size of a landing platform affixed to the vehicle, and the highly dynamic conditions in which deliveries may be accomplished, the control effort must be accurate and robust in the face of disturbances.

Fuzzy control is able to accommodate nonlinearities in the dynamic system such as are found in the situation of an air vehicle to ground transport rendezvous[15]. Current approaches for developing trajectory paths have focused on time-optimality[1][14] and not necessarily on lightweight, on-board controllers. In contrast, this work will

optimize for reduced control effort and computational simplicity and efficiency. The control developed in this will be largely agnostic to the large linearities inherent in the system dynamics and will apply linguistic variables and logic to intuitively attain the interception and landing. Accuracy will be paramount as the target platform is nearly equally-sized to the sUAV.

4.2 System Architecture

The research setup consists of a quadrotor aircraft of size 450 mm on the diagonal and a mobile rover robot with a 255 mm radius landing platform affixed to it (as shown in figure 4.1. The quadrotor is controlled by a Pixhawk flight controller which uses the PX4 flight control firmware. This flight controller allows for an on-board computer to take over control of the aircraft via a serial wire connection. A small Linux-based computer is placed on the quadrotor which sends velocity setpoints to the flight controller. All control logic is written in Python using a collection of softwares called Robot Operating System (ROS). ROS allows for easy integration of sensors and control actuation due to a distributed computation framework. As a highly event-driven, publish-subscribe model, ROS maintains an accurate, up-to-date view of internal states which are then exposed to any connected nodes.

An assumption is made that GPS (or some other global positioning) data is available for the simulation; however, this positioning has a margin of error which is far too large to be used exclusively for precision landing. For this reason, an on-board, camera will be utilized to detect and locate the target. Using the characteristics of the camera focal length and distortion coefficients, an accurate positional error can be obtained for the feedback control loop.

Figure 4.1: The test sUAV with the mobile target platform.

4.2.1 Onboard Software

ROS is an open source framework developed specifically to ease the development of software for robotics and robotics control[25]. Using ROS, it becomes a simple task to distribute computational loads across a computational graph of separate nodes. Additionally, ROS has a rich library of packages which are both useful for low-level processing of sensor information or managing hardware interfaces, and also high-level behavioral control or localization schemes. This project relies heavily on the work of many others in the area of visual odometry[24], kalman filtering[23], and flight control[11, 21]. The structure allows a roboticist to build and manage highly complex systems in a reliable way (see figure 4.2

Control of the quadcopter is handled in discrete stages based on vehicle state. It is assumed that the vehicle will have a rough estimate of the target location given to it so that it can travel to the appropriate region and find the target in the field of view of the camera sensor. Vehicle motion from arming until target location is handled by sending waypoints to the flight controller. Once the target is located in the image, The

vehicle gives control over to a set of FISs. The controller is described in more detail in section 4.4. The vehicle behavior over an entire mission is handled using a state machine[3]. Using a state machine allows the control to be handled in well-defined domains and ensures that transitions between states are handled smoothly. The states comprising a full mission from take to landing are shown in figure 4.3.

The state of the vehicle is managed by fusing together the positional estimate from the camera sensor and the AprilTag estimate (see section 4.4.1 as well as orientation information from the onboard IMU using an extended kalman filter (EKF). This estimate is only valid when the vehicle has a visual track on the target platform, otherwise, it is assumed that the vehicle is still in transit from its launch location, or it has landed. As can be seen in figure 4.3, the mission starts by arming the vehicle and immiediately sending the waypoint to approach the target area. When the vehicle enters the "TRACK" state, it is en route to the target location; while in this state, it monitors the quality of its visual estimation of the target location by evaluating the norm of the covariance matrix computed by the EKF. Only when the covariance is sufficently small does the vehicle transition to the next state.

The transition to the "APPROACH_LAND" state signals the transfer of control from the flight controller's waypoint manager to the FISs. While the vehicle is approaching and eventually landing on the target pad, a wrapping state monitors the state of the vehicle to calculate a fitness of the behavior. This fitness is returned to a master process which manages individual runs to execute the GA. In actual flight on hardware, the fitness process would be absent. When the vehicle meets a proximity threshold in the "APPROACH" state, it transitions to the "LAND" state and puts

down onto the landing pad. The details of the simulation, control, vision estimation, and devlopment process are discussed at length in the following sections.

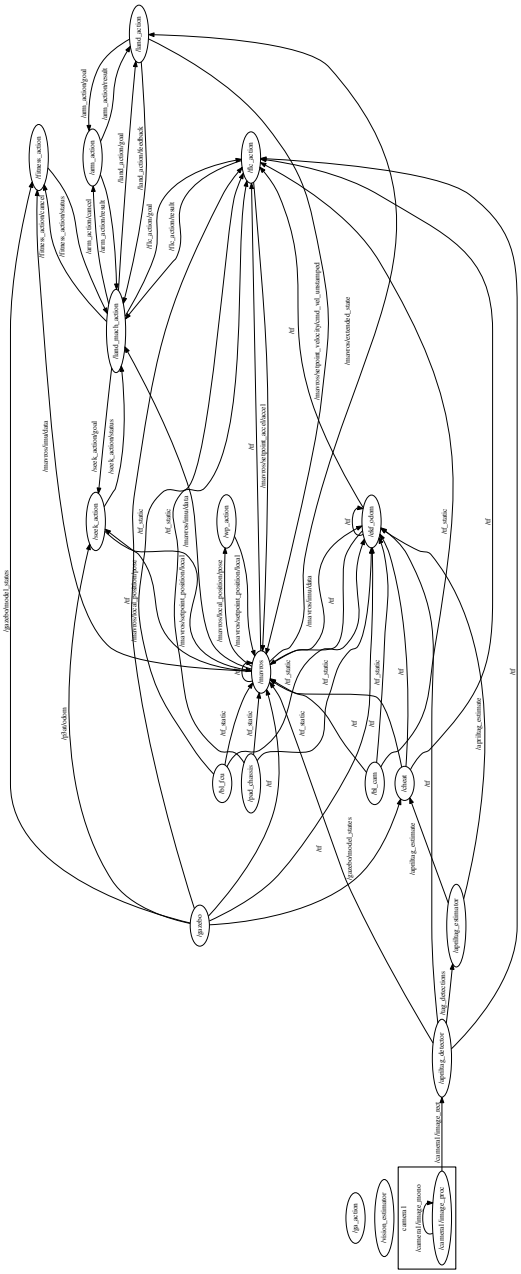

Figure 4.2: Sample compute graph for a single mission simulation. Note that each node in the graph represents a computational unit. The edges between nodes represent data sharing

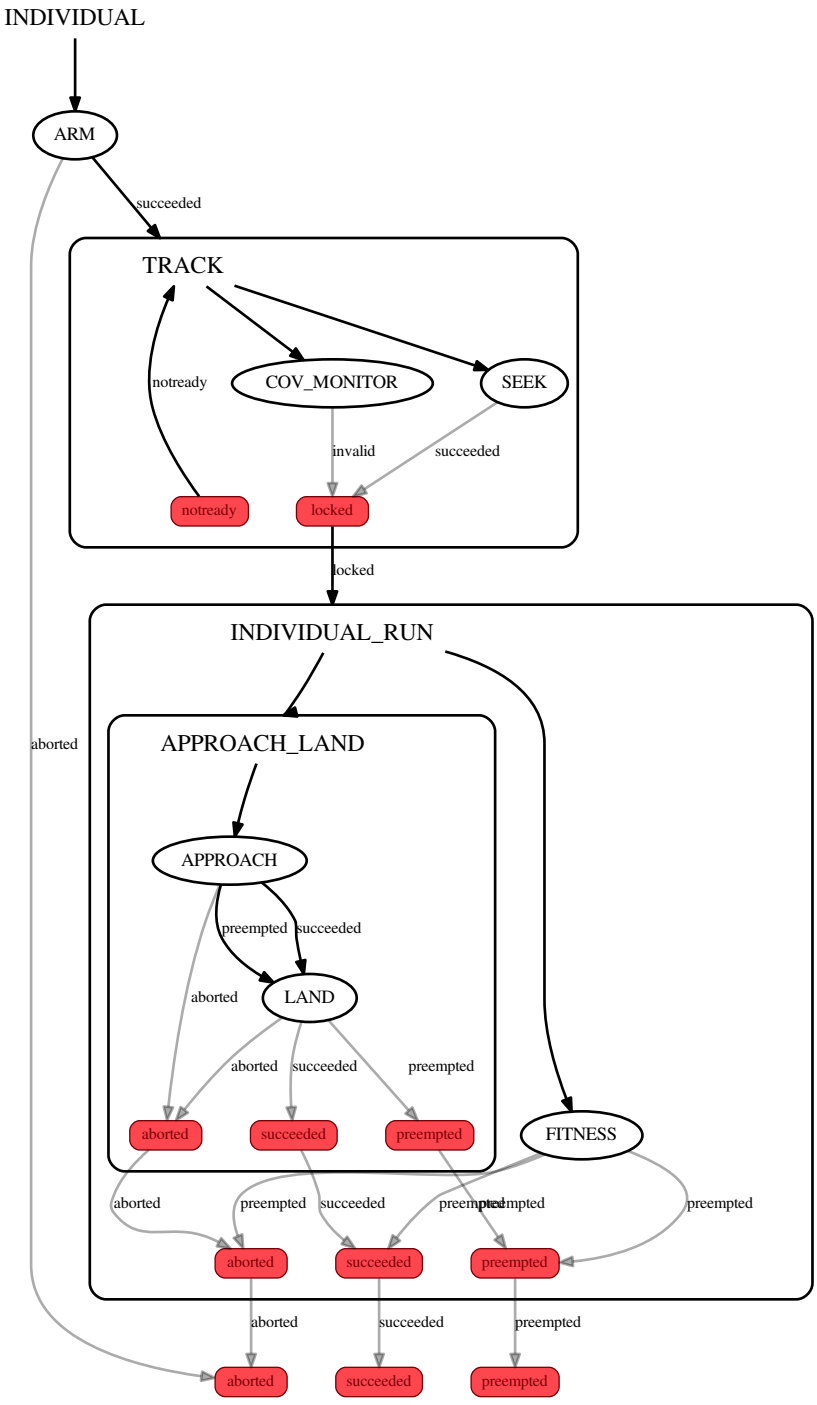

Figure 4.3: State machine of robotic lander

4.3 Simulation

Gazebo is a 3D simulation software which uses open source dynamics engines Bullet, Dart, and ODE to model its components. While Gazebo has very high fidelity simulation capabilities for robots (its initial purpose), the complexities of aerodynamics in general, and multicopter physics in particular, can only be modeled with many simplifications. Even with the simplified dynamics, the simulation environment that Gazebo provides is very useful for high-level controller development. Gazebo allows for the simulation of many sensor types and nicely integrates with ROS and the PX4 flight controller firmware. The high fidelity of the simulation will ease the transition from virtual to real flight as all hardware components have simulated counterparts. The simulation provides a real time interface for tuning the controller with visual feedback. This is the process which was used to tune the PID controller and will be used as well for the tuning of the fuzzy controller.

The most important aspect of sensing for the system is the image sensor. A camera sensor is simulated from the underside of the quadrotor to test the efficacy and efficiency of the computer vision algorithms. Care was taken to accurately represent the field of view and pixel noise of the physical camera sensor to be used. In this way, it is hoped that the controllers developed in simulation will be applicable on the physical system.

The high fidelity of the simulation comes with the drawback that it is only able to be run in real time, making training with a GA difficult to attain in any reasonable amount of time. Another drawback of accuracy is that simulation is that each individual sensor in the simulation is modeled with near-realistic noise values. This is by design in order to train a robust controller, but comes with the side effect that

no simulation run is perfectly repeatable. This introduces the frequent case that the top-performing controller from on GA generation may be a failure on the next due to either it being overtrained, or a case of bad luck. For this reason, the GA was never ver successful at training a controller which performed well consistently. In the end, a fuzzy controller was hand-tuned to meet the needs of the controller. Although the GA was never successful, much important information was gained in the process of making the attempt.

4.3.1 Fitness Function Development

The author was met with surprising difficulty in developing an effective cost function. Most attempts resulted in unintended consequences with minima resulting from non-optimal behavior. Finally the fitness function was broken into a behavioral fitness function (BFF) (equation (4.1)) to grade the action of the vehicle over time and an aggregate fitness function (AFF) (equation (4.2)) to measure the fitness of the final state of the vehicle. These are linearly combined to create a tailored fitness function (TFF)[8].

$$J_{bff} = \sum_{i=0} \left(\hat{p}_i \cdot \hat{v}_i + 1\right) \frac{t_i}{|t|} \tag{4.1}$$

$$J_{aff} = |p_f| \tag{4.2}$$

$$J_{tff} = J_{bff} J_{tff} \tag{4.3}$$

where $\hat{p}$ is the unit position vector of the vehicle with respect to the landing pad, $\hat{v}$ is the unit velocity vector, and the subscript i denotes a single instant in the time history. Note that the time must be normalized because the time taken for a full simulation from target track to landing will take a non-deterministic time. This scaling

by the time step serves the function of penalizing late-game mistakes greater than early errors; errors in the terminal stage of approach are more likely to abort the process, so require a stricter grading. This time-scaling requires that the BFF be computed post-facto as opposed to in real time.

4.4 Controller

Control is exerted on the vehicle by supplying the flight controller with changes in the velocities, Δv_x, Δv_y, and Δv_z, as well as yaw rate, $\dot{\psi}$. The quadrotor is able to land with any arbitrary yaw angle, ψ, but the assumption is made that some reception mechanism may expect the vehicle in a nose-forward orientation. Distance to the platform is estimated from images taken by the camera sensor. Orientation is estimated only in the last phase of the landing sequence using a robust and efficient visual fiducial tag system[24] (see figure 4.4).

4.4.1 Computer Vision

Much emphasis is put on the sensing algorithms to be computationally efficient to decrease the load on the on-board computer. For this purpose, only a small number of image processes are required to detect and locate the target. As a first pass, the image is brought into the Hue-Saturation-Value (HSV) color space. This has been shown to be a robust space in which do perform color detection and segmentation in uncontrolled and unpredictable lighting conditions[32]. A simple thresholding is performed on the image to isolate a sufficiently wide band of yellows to match the color of the target and dilate this to a binary blob. From this binary image, the image moments are calculated by

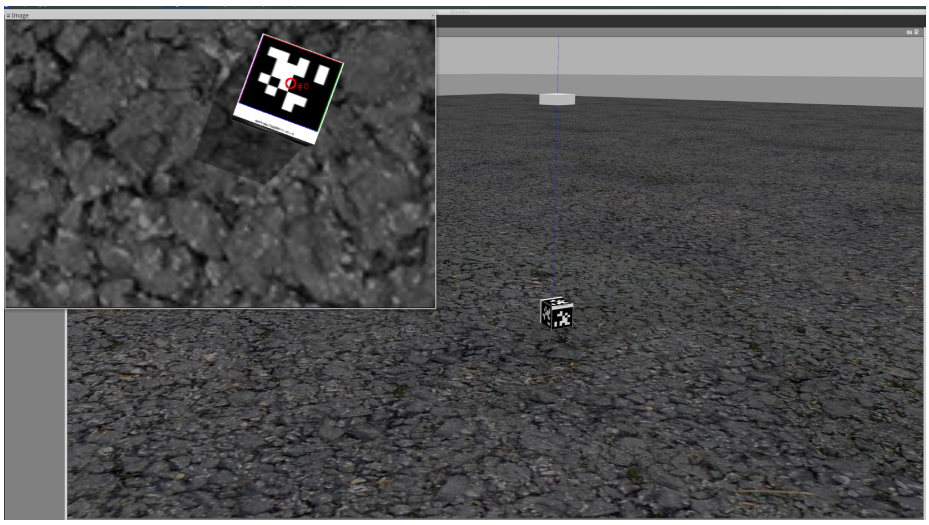

Figure 4.4: Simulated image sensor detection of AprilTag marker.

$$m_{ij} = \sum_{x,y} x^i y^j I_{xy} \tag{4.4}$$

where I_{xy} is the pixel intensity value for each pixel (x, y) (equal to 1 in this case) and $i, j = 0, 1, 2$. From this it can be seen that m_{00} describes the area and $\frac{m_{10}}{m_{00}}$ and $\frac{m_{01}}{m_{00}}$ describe the centroids $\overline{x}_p$ and $\overline{y}_p$ in terms of pixels. The blob is assumed to be circular and hence a diameter is extracted from the pixel area. Using the focal length of the sensor, these image points are then projected onto the ground plane using the known diameter of the landing pad and a vertical offset estimate is obtained as is shown in equation (4.5).

$$d_z = \frac{d \cdot f}{m \cdot d_p} \tag{4.5}$$

where f is the focal length of the camera in units of length, d is the known diameter of the landing pad, d_p is the estimated diameter in pixels, and m represents a scaling factor in units of $\frac{\text{pixel}}{\text{mm}}$ (unity in the simulation). Assuming that the image plane and

the ground plane are parallel, the center of the image can be assumed to point directly below the vehicle and the horizontal offsets to the landing pad can then be calculated as

$$d_x = d_z \cdot \frac{m\bar{x}_p}{f} \tag{4.6}$$

$$d_y = d_z \cdot \frac{m\bar{y}_p}{f} \tag{4.7}$$

As the vehicle approaches the landing pad, the image field of view is overtaken by the landing pad itself and the former segmentation no longer becomes effective. For this purpose, an apriltag[24] (see figure 4.4) is placed on the center of the target. Once detection of this tag is achieved, an refined estimate of position and even orientation is obtained with respect to the target. This estimate is used to then orient the vehicle to match the heading of the landing pad (see figure 4.5).

4.4.2 PID Results

A PID controller was created which uses the most recent error estimates and sends velocity requests to the flight controller. Due to the lack of a mathematical model of the system. The PID gains were found by iterating the simulation with various position setpoints and dynamically adjusting the gains while observing the response visually. This closely mimics the method by which PID gains are attained in the tuning of an actual quadrotor by flying a series of test flights and adjusting gain values by feel. In this way, a reasonable response and landing sequence was achieved for first a static target and then repeated for a dynamic target moving with constant velocity. The results are presented in figures 4.7(a) to 4.7(b) in which the normed horizontal offset from target is shown in conjunction with the vertical distance to the platform.

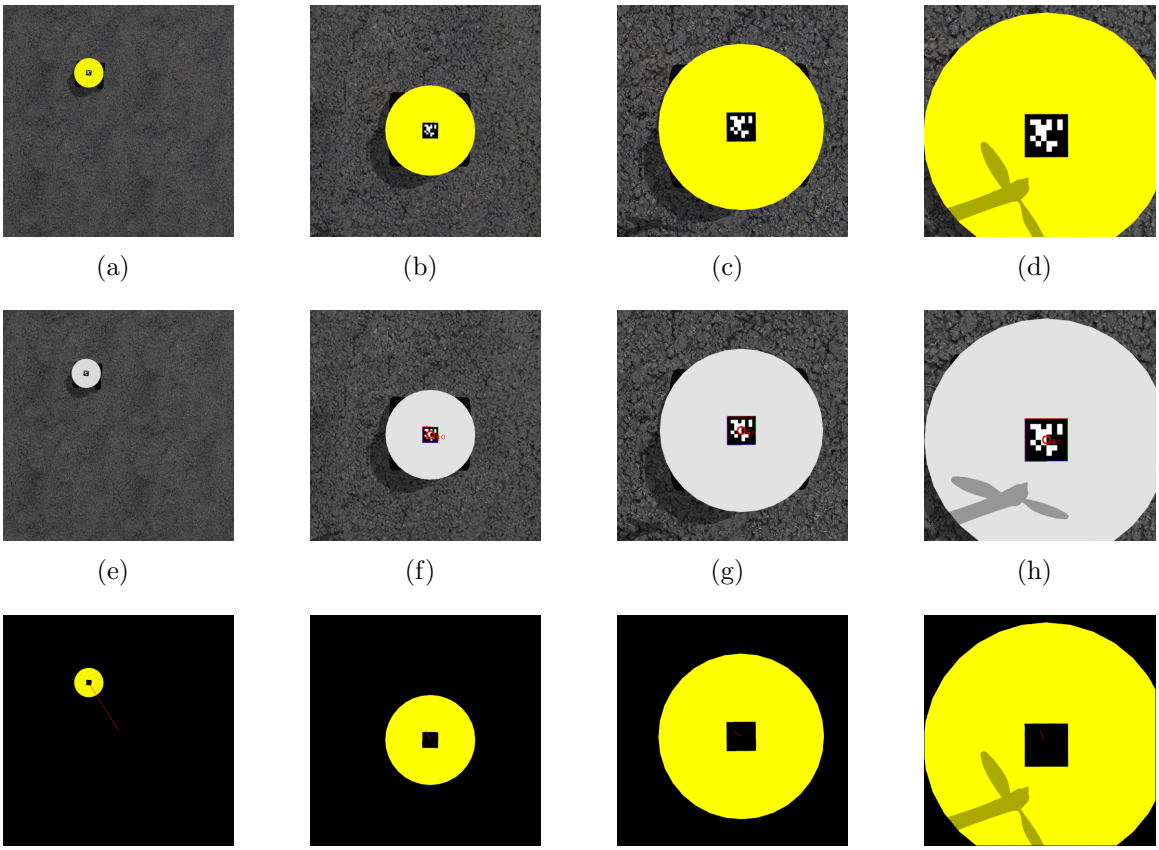

Figure 4.5: A time series of images taken during the landing maneuver. Note that in figure 4.5(e), there is no detection of the marker and there remains a slight error in yaw angle as a result. The red line in figures 4.5(i) to 4.5(l) represents the horizontal offset of the vehicle to the desired point on the target.

Viewing the charts, it is apparent that as the vehicle approaches the target, it tends to accumulate horizontal errors and must correct more frequently, particularly in the dynamic case. In both cases, the quadrotor managed to successfully land on the target. In the static case, the final offset from the center of the target was less than 5 cm. For the dynamic case, the error was 7 cm which nearly displaced it from the target surface. In both cases, the sink rate and yaw rates were controlled by simple PD controllers.

4.4.3 Fuzzy Results

Though this work is still in progress, promising preliminary results in development of a fuzzy controller have been obtained. Four fuzzy controllers of similar architecture were created as shown in figure 4.6. Each input fuzzy partition was multiplied by a scaling factor to bring it into the regime of the controller. Likewise, the outputs were then again scaled to match actuation limits. The rule base was developed using common intuition about the system dynamics. A full rule matrix was defined to fully cover the system possibilities. This rule matrix is shown in table 4.1. The rules are made up of linguistic variables composed into IF-THEN constructions of antecedents and consequents. For example:

$$\text{IF } \textit{error} \text{ is } \mathbf{N} \text{ AND } \textit{error rate} \text{ is } \mathbf{Z} \text{ THEN } \Delta v \text{ is } \mathbf{SP}$$

These rules are intuitive and easy to understand and provide a process by which to lend the controller a decision-making system with a foundation in human reasoning. The tuning process of the fuzzy controller then becomes the task of defining the membership functions which decide how much of each rule should be activated for certain inputs. Triangular membership functions are used exclusively for their simplicity in definition and tuning[22] while the aggregation of rules is the popular

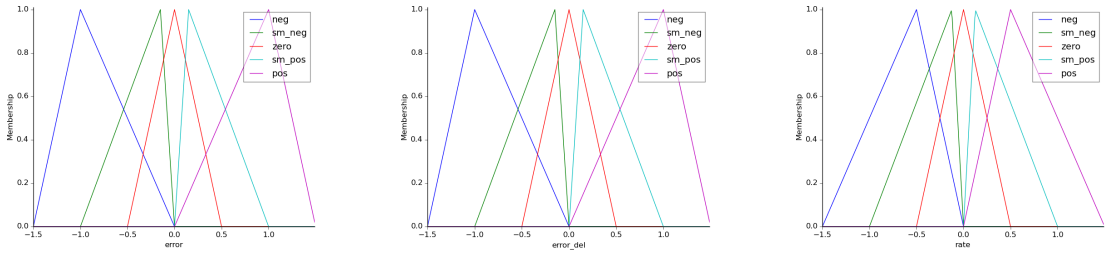

(a) Fuzzy input partition template (b) Fuzzy input partition template (c) Fuzzy output partition template

Figure 4.6: Membership function definitions for fuzzy logic controller.

min-max method put forth by Mamdani[19]. The membership functions shown in figure 4.6 are the result of only a small number of iterative tuning steps and were found to be the most effective of the configurations attempted. The fuzzy rule base also provides ample opportunities for tuning and will have a significant impact on controller performance.

Table 4.1: Fuzzy rule base

		error				
		N	SN	Z	SP	P
error rate	N	P	P	SP	SP	Z
	SN	P	SP	SP	Z	SN
	Z	SP	SP	Z	SN	SN
	SP	SP	Z	SN	SN	N
	P	Z	SN	SN	N	N

The result of this first-iteration controller was sufficient to land the quadrotor on both the static and constant linear velocity dynamic platforms, though the response to uncertainties is not very stable as of yet. The results shown in figures 4.8(a) to 4.8(b)

demonstrate the difficulty an untrained controller may have with novel situations. The results are expected to improve dramatically by using genetic algorithms to tune each controller.

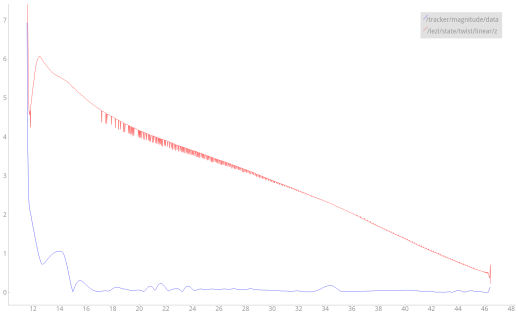

(a) $(kp, ki, kd) = (2.1, 0.015, 0.2)$ for static target interception.

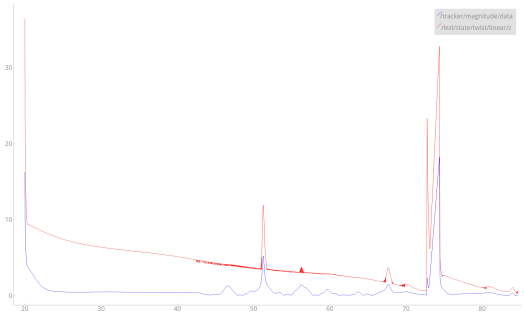

(b) $(k_p, k_i, k_d) = (1.8, 0.012, 0.02)$ for dynamic target interception.

Figure 4.7: PID controllers for static and dynamic landing

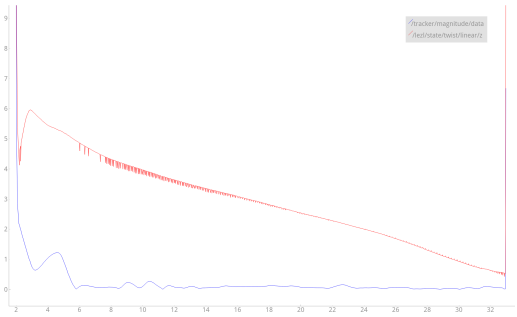

(a) Static target interception.

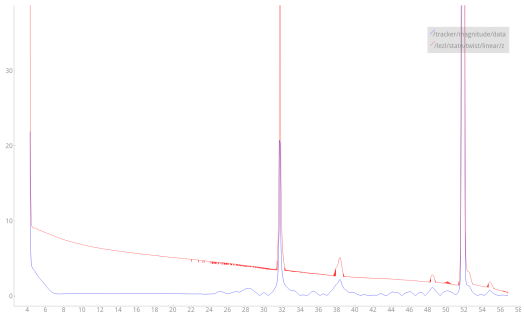

(b) Dynamic target interception.

Figure 4.8: Fuzzy controllers for static and dynamic landing

4.5 Conclusion

The results presented are preliminary only, but show promising results. The control effort of the untuned fuzzy controller nearly matched that of the tuned PID controller for the static target case. For the dynamic target, while neither controller was tuned to any high degree of accuracy, the fuzzy controller performed at least as well as the PID controller. It should be noted that the overall positioning control of the vehicle is relatively simple, but as it approaches more closely to the platform, small movements are translated to larger apparent errors and the controller may make bad decisions. This explains the peaks which can be seen in both of the dynamic situations; as the quadrotor becomes very near to the platform, it occasionally loses visual sight of the key target and must then abort the landing and gain altitude to retry.

There is much future work to yet complete. Both the PID and Fuzzy controllers will be tuned by a genetic algorithm which will greatly improve the performance of each. To prepare the system for real world deployment, the perfect gimbal assumption being made in the simulation will be replaced with a rigidly mounted camera. This will require then applying a rotational transform to each image pixel measurement which will increase the uncertainty in each estimate. Finally, the image processing pipeline must be optimized even further to decrease the computation load on the processor. With the current pipeline, the test hardware processes images at around 2 Hz, which may introduce too much latency in the control feedback. Either the image processing must be sped up, or the delay will need to be handled in some other fashion.

Chapter 5: Conclusions

Appendix A: C Genetic Fuzzy Library Documentation

Appendix B: Python Genetic Fuzzy Library Documentation

Bibliography

[1] Jerrod C. Adams. An interpolation approach to optimal trajectory planning for helicopter unmanned aerial vehicles. Master's thesis, Naval Postgraduate School, Monterey, California, 6 2012.

[2] Ulrich Bodenhofer and Francisco Herrera. Ten lectures on genetic fuzzy systems. *Preprints of the International Summer School: Advanced Control-Fuzzy, Neural, Genetic*, pages 1–69, 1997.

[3] Jonathan Bohren and Steve Cousins. The smach high-level executive [ros news]. *IEEE Robotics & Automation Magazine*, 17(4):18–20, 2010.

[4] David Bossert and Kelly Cohen. Pid and fuzzy logic pitch attitude hold systems for a fighter jet. In *AIAA Guidance, Navigation, and Control Conference and Exhibit*, page 4646, 2002.

[5] UK Chakraborty and DG Dastidar. Chromosomal encoding in genetic adaptive search. In *Proc. Intl Conf. on Signals, Data and Systems, AMSE*, volume 2, pages 191–195, 1991.

[6] K. Cohen, T. Weller, and J.Z. Ben-Asher. Control of linear second-order systems by fuzzy logic-based algorithm. *Journal of Guidance, Control, and Dynamics*, 24(3):494–501, 2001.

[7] O. Cordón, F. Herrera, F. Hoffmann, and L. Magdalena. *Genetic Fuzzy Systems, Evolutionary Tuning and Learning of Fuzzy Knowledge Bases*. World Scientific Publishing Co., MA, 2001.

[8] Mohammad Divband Soorati and Heiko Hamann. The effect of fitness function design on performance in evolutionary robotics: The influence of a priori knowledge. In *Proceedings of the 2015 Annual Conference on Genetic and Evolutionary Computation*, pages 153–160. ACM, 2015.

[9] Yinpeng Dong, Hang Su, Jun Zhu, and Bo Zhang. Improving interpretability of deep neural networks with semantic information. *arXiv preprint arXiv:1703.04096*, 2017.

[10] Nicholas Ernest, Kelly Cohen, Elad Kivelevitch, Corey Schumacher, and David Casbeer. Genetic fuzzy trees and their application towards autonomous training and control of a squadron of unmanned combat aerial vehicles. *Unmanned Systems*, 3(03):185–204, 2015.

[11] Fadri Furrer, Michael Burri, Markus Achtelik, and Roland Siegwart. Robot operating system (ros). *Studies Comp.Intelligence Volume Number:625*, The Complete Reference (Volume 1)(978-3-319-26052-5):Chapter 23, 2016. ISBN:978-3-319-26052-5.

[12] Ian Goodfellow, Yoshua Bengio, and Aaron Courville. *Deep Learning*. MIT Press, 2016. `http://www.deeplearningbook.org`.

[13] Nikolaus Hansen and Andreas Ostermeier. Convergence properties of evolution strategies with the derandomized covariance matrix adaptation: The (=. *Eufit*, 97:650–654, 1997.

[14] Markus Hehn and Raffaello D'Andrea. Real-time trajectory generation for interception maneuvers with quadrocopters. In *2012 IEEE/RSJ International Conference on Intelligent Robots and Systems*. Institute of Electrical & Electronics Engineers (IEEE), oct 2012.

[15] S. Ionita. A fuzzy approach on guiding model for interception flight. In *Fuzzy Systems Engineering*, pages 85–111. Springer Science & Business Media, Jul 2005.

[16] B. Kosko and S. Isaka. Fuzzy logic. *Scientific American*, 269(1):76–81, 1993.

[17] Bart Kosko. *Fuzzy Thinking, The New Sciencs of Fuzzy Logic*. Hyperion, NY, 1994.

[18] Zachary C Lipton. The mythos of model interpretability. *arXiv preprint arXiv:1606.03490*, 2016.

[19] E.H. Mamdani and S. Assilian. An experiment in linguistic synthesis with a fuzzy logic controller. *International Journal of Man-Machine Studies*, 7(1):1 – 13, 1975.

[20] The MathWorks Inc, Natick, Massachusetts, United States. *MATLAB and Fuzzy Logic Toolbox Release 2012b*, 2012.

[21] Lorenz Meier, Dominik Honegger, and Marc Pollefeys. Px4: A node-based multithreaded open source robotics framework for deeply embedded platforms. In *Robotics and Automation (ICRA), 2015 IEEE International Conference on*, pages 6235–6240. IEEE, 2015.

[22] SK Mishra, IG Sarma, and KN Swamy. Performance evaluation of two fuzzy-logic-based homing guidance schemes. *Journal of Guidance, Control, and Dynamics*, 17(6):1389–1391, 1994.

[23] T. Moore and D. Stouch. A generalized extended kalman filter implementation for the robot operating system. In *Proceedings of the 13th International Conference on Intelligent Autonomous Systems (IAS-13)*. Springer, July 2014.

[24] Edwin Olson. AprilTag: A robust and flexible visual fiducial system. In *Proceedings of the IEEE International Conference on Robotics and Automation (ICRA)*, pages 3400–3407. IEEE, May 2011.

[25] Morgan Quigley, Ken Conley, Brian Gerkey, Josh Faust, Tully Foote, Jeremy Leibs, Rob Wheeler, and Andrew Y Ng. Ros: an open-source robot operating system. In *ICRA workshop on open source software*, volume 3, page 5. Kobe, Japan, 2009.

[26] Marco Tulio Ribeiro, Sameer Singh, and Carlos Guestrin. Why should i trust you?: Explaining the predictions of any classifier. In *Proceedings of the 22nd ACM SIGKDD International Conference on Knowledge Discovery and Data Mining*, pages 1135–1144. ACM, 2016.

[27] Tim Salimans, Jonathan Ho, Xi Chen, and Ilya Sutskever. Evolution strategies as a scalable alternative to reinforcement learning. *arXiv preprint arXiv:1703.03864*, 2017.

[28] Robert F Stengel and Christopher I Marrison. Robustness of solutions to a benchmark control problem. *Journal of Guidance, Control, and Dynamics*, 15(5):1060–1067, 1992.

[29] Bong Wie and Dennis S Bernstein. Benchmark problems for robust control design. *Journal of Guidance, Control, and Dynamics*, 15(5):1057–1059, 1992.

[30] L.A. Zadeh. Fuzzy sets. *Information and Control*, 8(3):338 – 353, 1965.

[31] Matthew D Zeiler and Rob Fergus. Visualizing and understanding convolutional networks. In *European conference on computer vision*, pages 818–833. Springer, 2014.

[32] Ming Zhao, Jiajun Bu, and Chun Chen. Robust background subtraction in hsv color space. In *ITCom 2002: The Convergence of Information Technologies and Communications*, pages 325–332. International Society for Optics and Photonics, 2002.